Regulation of Pannexin 1 and Pannexin 3 during Skeletal Muscle Development, Regeneration, and Dystrophy

Tammy Pham

This thesis is submitted to the Faculty of Graduate and Postdoctoral Studies as a partial fulfillment of the M.Sc. program in Cellular Molecular Medicine

Date: January 20, 2018

Department of Cellular and Molecular Medicine

Faculty of Medicine

University of Ottawa

451 Smyth Road, Rm 3206

Ottawa, ON K1H 8M5

ABSTRACT

Pannexin 1 (Panx1) and Pannexin 3 (Panx3) are single membrane channels recently implicated in myogenic commitment, as well as myoblast proliferation and differentiation *in vitro*. However, their expression patterns during skeletal muscle development and regeneration have yet to be investigated. Here, I show that Panx1 levels increase during development, becoming highly expressed in adult skeletal muscle. A switch in Panx3 expression pattern was observed as its ~70 kDa immunoreactive species was mainly expressed in embryonal and neonatal muscles while its ~40 kDa species was the main form expressed in adult skeletal muscle. In adult mice, Panx1 and Panx3 were differentially expressed in fast- and slow-twitch muscles. Interestingly, Panx1 and Panx3 levels were modulated in muscle degeneration/regeneration, similar to the pattern seen during skeletal muscle development. Since Duchenne muscular dystrophy is characterized by skeletal muscle degeneration and impaired regeneration, I next used mild and severe mouse models of this disease and found a significant down-regulation of both Panx1 and the lower MM form of Panx3 in dystrophic skeletal muscles, with an increase in the ~70 kDa immunoreactive species of Panx3. I also found that Panx1/PANX1 and Panx3/PANX3 are co-expressed in mouse and human satellite cells, which play crucial roles in skeletal muscle regeneration. Indeed, *in vitro* PANX1 levels may be increasing during human primary satellite cell differentiation and blocking PANX1 channel activity with the pharmacological compounds probenecid or carbenoxolone inhibited the differentiation and fusion of these satellite cells into myotubes. In addition, satellite cell proliferation was inhibited by probenecid and carbenoxolone. These findings are the first to demonstrate that Panx1 and Panx3 are

differentially expressed amongst skeletal muscle types with their levels being highly modulated during skeletal muscle development, regeneration and dystrophy. In addition to our laboratory's previous reports, I now demonstrate that PANX1 levels may be modulated during satellite cell differentiation and that PANX1 channels regulate satellite cell differentiation and proliferation. Altogether, my studies suggest that Panx1/PANX1 and Panx3/PANX3 channels may play important and distinct roles in myoblasts and satellite cells in healthy and diseased skeletal muscles.

ACKNOWLEDGEMENTS

I would like to thank my supervisor, Dr. Kyle Cowan, as well as Dr. Stephanie Langlois for providing me with this excellent opportunity and for sharing their genuine passion for science and their dedication to furthering the growth of their students. I am also thankful to thesis advisors Dr. Bernard Jasmin and Dr. Alex Mackenzie for their guidance and support throughout my degree. Finally, I am grateful to have been a part of the amazing community that is the CHEO Research Institute that includes my lab members, and all other staff and students.

TABLE OF CONTENTS

LIST OF FIGURES

LIST OF ABBREVIATIONS

aa – amino acids

ATP – adenosine triphosphate

BrdU - bromodeoxyuridine

BSA – bovine serum albumin

Cas - Clustered Regularly Interspaced Shot Palindromic Repeats-associated proteins

Cav-1 – caveolin-1

$Ca_v1.1$ – voltage sensor dihydropyridine receptor

CRISPR – Clustered Regularly Interspaced Shot Palindromic Repeats

CTX – cardiotoxin

DHPR – dihydropyridine receptor

dKO – double knockout

DMD – Duchenne muscular dystrophy

DMEM – Dulbecco Modified Eagle's medium

DNA – deoxyribonucleic acid

ER – endoplasmic reticulum

EDL – *extensor digitorum longus*

ELISA – enzyme-linked immunosorbent assay

ERK – extracellular signal-regulated kinase

E-T coupling – excitation-transcription coupling

FBS – fetal bovine serum

GAPDH – glyceraldehyde 3-phosphate dehydrogenase

H&E – hematoxylin and eosin

HEK – human embryonic kidney

HSMM – Primary Human Skeletal Muscle Myoblasts

kDa – kilodaltons

KO - knockout

MHC – myosin heavy chain

MM – molecular mass

MRF – myogenic regulatory factors

MYOG - myogenin

Panx/PANX – Pannexin

PBS – phosphate-buffered solution

PCR – polymerase chain reaction

RC – reserve cells

RNA – ribonucleic acid

ROS – reactive oxygen species

RPS6 – ribosomal protein S6

SC – satellite cell

SDS-PAGE – sodium dodecyl sulfate-polyacrylamide gel electrophoresis

SkMCM – Skeletal Muscle Cell Medium

SOL - *soleus*

TA – *tibialis anterior*

TnI – troponin

µm - micrometre

1.0 INTRODUCTION

1.1 Pannexin Overview

The pannexin (Panx) family of proteins consists of single membrane channels that were reported for the first time in 2000 [1]. There are three known members in the mammalian genome: Panx1, Panx2 and Panx3. Panx1 is ubiquitously expressed in various organs and tissues such as the brain, skin, heart, bone, lung, and elements of the immune system including macrophages [2–8]. Panx2 was first reported to have restricted expression to the central nervous system [9,10], but a more recent report suggests that its endogenous expression may be more ubiquitous [11]. Current literature reports Panx3 being abundant in adult skin [5], bone [12], cartilage [13], as well as skeletal muscle [14].

Looking at the amino acid (aa) sequences of Panx1 (426 aa), Panx2 (677 aa) and Panx3 (392 aa), they are well-conserved with >70% identity and >80% similarity across various animal species [3,15–18]. Interestingly, Panx1 and Panx3 paralogs are relatively well-conserved sharing ~60% identity and ~75% similarity, while Panx2 demonstrates significant sequence divergence from the other Panx family members [18]. This thesis will focus mostly on Panx1 and Panx3, as these are co-expressed in skeletal muscle, while Panx2 protein was not detected in this tissue [14]. At the secondary structure level, Panx glycoproteins are predicted to constitute four α-helical transmembrane domains, two extracellular loops, one intracellular loop, and cytoplasmic amino and carboxyl termini [1,3,19,20]. Panx1 oligomerize into a hexamer to form single membrane channels, while Panx3 is predicted to also form hexamers based on its sequence similarity to Panx1 [21].

Panx1 and Panx3 glycosylated species are detected between ~37 and 50 kDa [4]. An immunoreactive species of Panx3 (~70 kDa) has also been reported and detected in murine skin, cartilage, ventricle, lung, liver, kidney, thymus, spleen, male reproductive tract, skeletal muscle [4,14,16,22] and human skeletal muscle [14]. While the exact identity of the ~70 kDa immunoreactive species of Panx3 remains unknown, it has been confirmed to be a glycoprotein and can be detected by different antibodies against Panx3 [14,22]. In addition, shRNAs against Panx3 successfully knocked down its levels [14], altogether suggesting that this ~70 kDa immunoreactive species likely corresponds to a Panx3 isoform.

Panxs are heavily glycosylated, generating distinct species with various molecular weights. Panx1 and Panx3 each have specific N-linked glycosylation sites: Panx1 is glycosylated on the second extracellular loop at asparagine 254, while Panx3 is glycosylated in the first extracellular loop at asparagine 71 [4]. In site-directed mutagenesis experiments, N-glycosylation-defective mutants of Panx1 and Panx3 were still able to traffic to the plasma membrane; however, there was an increase in their intracellular localization compared to wild-type Panx1 and Panx3 [4]. Thus, the glycosylation status of Panx1 and Panx3 may play a role in their trafficking to the cell surface. The level of N-glycosylation also governs the intermixing of Panx family members to form heterogeneous channel proteins where the most highly glycosylated species do not participate in intermixing [4,21,23].This intermixing is most evidently observed between Panx1 and Panx2 leading to compromised channel activity [23,24]. Panx1 and Panx3 intermix to a lesser extent with no observed change in channel function [23]. Panx2 and Panx3 do not intermix at the biochemical level [23], and there are no reports about their

intermixing in cells or tissues. This relationship between the glycosylation pattern of Panx1 and Panx3 and their trafficking to the cell membrane and intermixing may in part regulate Panx channel functions.

Panx channel functions include ATP release to the extracellular space or Ca^{2+} release from the endoplasmic reticulum (ER) [20]. For example, Panx1 as a single membrane channel at the cell membrane can release ATP into the extracellular space to elicit Ca^{2+} wave signalling via P_2X_7 receptor activation [8,25,26]. Binding of extracellular ATP and ADP to purinergic P_2Y receptors increases the levels of inositol 1,4,5-triphosphate (IP_3), which signals intracellular increase of Ca^{2+} levels by releasing Ca^{2+} from ER stores [8,25,26]. This accumulation of intracellular Ca^{2+} signals to Panx1 single membrane channels further stimulate ATP release and propagation of signals to neighbouring cells [8,25,26]. Less extensively studied is the Panx1 potential to uptake glucose during skeletal muscle contraction [27]. Conversely, Panx3 has been proposed to act as an ATP channel at the cell membrane as well as a Ca^{2+} channel in the ER of C_2C_{12} cells and primary calvarial osteoblasts during their differentiation [28].

All Panx channels are capable of dye uptake [4,23,29]. Both Panx1 and Panx3 channels are activated by mechanical stimulation and extracellular ATP [4,8,25,28,30,31]. Panx1 channels are also stimulated by membrane depolarization, caspase cleavage, cytoplasmic Ca^{2+} often through G-coupled P_2Y_1/P_2Y_2 receptors or purinergic P_2X_7 receptors, extracellular K^+, or glutamate via NMDA receptors [4,30–35]. Panx1 channel function has been shown to be inhibited by negative feedback from ATP release [30], CO_2-mediated cytoplasmic acidification [30], mimetic peptides such as ^{10}PANX1 [36,37], and

pharmacological compounds such as probenecid, carbenoxolone and flufenamic acid [24,38,39].

Panx1 channels have been implicated in various cellular and physiological processes such as Ca^{2+}-wave propagation, stabilization of synaptic plasticity and learning, vasodilation, inflammatory responses, apoptosis, epithelial progenitor proliferation, and keratinocyte differentiation [5,25,34,40–45]. On the other hand, there is less knowledge surrounding the cellular and physiological functions of Panx3. Panx3 channels have been reported to regulate the differentiation and proliferation of chondrocytes, osteoblasts, osteoprogenitors, myoblasts [13,14,28], and is required for normal muscle development [46,47].

There are only a couple of reports where mutations in pannexin-encoding genes led to human diseases. In one case report, a young female possessed a homozygous PANX1 variant that was associated to multisystem dysfunction which included skeletal defects [48]. In another report that screened highly metastatic breast cancer cell lines, a mutation leading to a truncated form of PANX1, "$PANX^{1\text{-}89}$", was highly enriched in these cancer cells allowing for their metastatic spread [49]. Moreover, there are many reports in the literature where pannexin over-expression or down-regulation *in vitro* and/or *in vivo* has been linked to disease onset and/or progression. Panx1 channels have been reported to play roles in epilepsy, multiple sclerosis, neuronal death during ischemia and stroke, death of enteric neurons during colitis, psychiatric conditions with cognitive dysfunction, Crohn's disease, and carcinogenesis [20,22,29,50–55]. Dysregulated Panx3 expression has been implicated in the biology of osteoarthritis, keratinocyte tumours, as well as carcinogenesis susceptibility linked to body mass index [5,22,56,57]. In summary,

there is a growing body of evidence that Panx1 and Panx3 channel activity play roles in many cellular and physiological functions as well as in disease states.

1.2 Skeletal Muscle Development

In vertebrates, the processes of myoblast proliferation and differentiation are crucial for muscle development as embryonic muscle mass increases predominantly by the proliferative growth of myoblasts, which eventually differentiate and fuse to form single-celled multi-nucleated myotubes and multi-nucleated myofibers [58,59]. Myoblasts are myogenic progenitor cells expressing MyoD and/or Myf5 and are capable of proliferating or exiting from the cell cycle during differentiation [60,61]. Satellite cells (SCs) are resident skeletal muscle stem cells distinct from embryonic myoblasts and have a larger role during skeletal muscle regeneration [61–67]. Proliferative myoblasts as well as SCs can be traced back to their embryonic source during somitogenesis of the mesoderm [68]. It is the dermomyotome layer developing from the somites that releases premyogenic precursors which migrate to the limb buds where they give rise to the majority of endothelia and skeletal muscle during fetal and postnatal development [69]. The migration of these delaminating cells from the dermomyotome is in large part regulated by the paired box transcription factor Pax3 which is necessary for myogenic specification [70–72]. As Pax3 is down-regulated through the increasing expression and action of myogenic regulatory factors (MRFs) such as MyoD, a family of basic helix-loop-helix transcription factors crucial to myogenesis, these pre-myogenic precursors become myoblasts at the limb bud [73]. In response to certain microenvironmental changes during development, the myoblasts leave the cell cycle and begin to differentiate and fuse into myotubes, as observed by the continued expression of MyoD together with the onset of myogenin

expression, among other MRFs, and a cell surface protein called myomaker [74,75]. The microenvironmental changes include the depletion of fibroblast growth factor, accumulation of sonic hedgehog and Wnt signalling molecules, and activation of serum response transcription factor [76–80]. Upon the expression of myosin heavy chain (MHC), myotubes and myofibers are terminally differentiated and found mostly in quiescent skeletal muscle at the end of postnatal period and in the adult [81].

Early embryonic stage in mice is considered E10.5-12.5, while fetal stage is E14.5-17.5. Starting in late embryonic development (E17.5), SCs are morphologically distinguishable from other cell types and skeletal muscle can be delineated based on various histochemical, biochemical, morphological and physiological features [82,83]. For example, fast- and slow-twitch muscle fibers are defined based on contractile speed, while types 1, 2A, 2X, and 2B are distinguished based on the MHC isoform expressed [84]. Type 1 fibers are predominantly found in slow-twitch muscles, while types 2A and 2B are abundantly present in fast-twitch muscles [85,86]. Furthermore, type 1 fibers tend to rely more on oxidative metabolism, while type 2B fibers are abundant in glycolytic enzymes. Interestingly, type 2A is classified as a hybrid oxidative glycolytic fiber [87]. Four skeletal muscle tissues are studied in this research: *tibialis anterior* (TA), which is composed of mostly of fast-twitch fibers; *extensor digitorum longus* (EDL), which has a mix of fast- and slow-twitch fibers; *soleus* (SOL), which is made of mostly slow-twitch fibers [88,89], and diaphragm (DPH), which is predominantly fast-twitch in mice but slow-twitch in humans due to their size [90,91].

1.3 Skeletal Muscle Regeneration

In adulthood, skeletal muscle is mostly quiescent except during skeletal muscle regeneration where SCs are the crucial players involved. In normal conditions, SCs quiescently reside in the niche under the basal lamina but they become activated during regeneration. Indeed, upon injury and skeletal muscle degeneration (usually via damage to the sarcolemma), myofiber permeability increases as reflected by the release of skeletal muscle proteins such as serum creatine kinase and by the influx of calcium [92–94]. Furthermore, inflammatory response factors such as neutrophils and later macrophages are activated and infiltrate the area. These inflammatory cells along with several growth factors released at the site of injury such as fibroblast growth factor and hepatocyte growth factor play a part in activating and attracting SCs via chemotaxis [95–102]. Intrinsically, SCs are activated in part through the transcriptional activity of Pax7 and up-regulation of MyoD, which indicate activated and proliferative SCs or SC-derived myoblasts [103]. Upon down-regulation of Pax7 and the increasing expression of myogenin, these cells become committed to terminal differentiation [103,104]. To note, Pax7 is crucial not only for myogenic commitment, but also for cell survival, self-renewal, and maintenance of SCs [105–107]. Indeed, *Pax7* KO mice show progressive loss of SCs, impaired regeneration, and skeletal muscle atrophy [108]. Early skeletal muscle regeneration is thus mostly characterized by fiber necrosis and extensive infiltration of inflammatory mononucleic cells [61,102]. In the second phase of skeletal muscle regeneration, expansion and differentiation of the activated SCs allow for restoration of the muscle mass as a subpopulation of these activated SCs will differentiate into fusion-competent myoblasts. These myoblasts can fuse to damaged fibers or fuse together to form new myotubes in a

process comparable to embryonic myogenesis although there is some controversy on the degree of similarity between embryonic and adult myogenesis [61,109,110].

SCs can maintain its pool through symmetric or asymmetric division during skeletal muscle regeneration. For example, when symmetric division is observed in $Pax7^{+}/Myf5^{+}$ cells, two daughter stem cells are generated where both maintain Pax7 and Myf5 expression [111]. In the asymmetrically-dividing SC, it is thought that differences in the microenvironment and asymmetric distribution of intracellular factors affecting certain myogenic genes determines the fate of the daughter cells – one commits to the myoblast lineage while the other becomes the quiescent daughter SC as a reserve for future muscle regeneration [111]. Extrinsic factors are usually distinguished by one daughter cell being exposed to the basal lamina microenvironment to likely re-enter quiescence, while the other daughter cell experiences the microenvironment of the myofibers plasma membrane to be pushed towards the myogenic lineage [112]. In an example of intrinsic factors directing SC asymmetric division, a $Pax7^{+}/Myf^{-}$ SC can generate a $Pax7^{+}/Myf^{-}$ SC stem cell alongside a $Pax7^{+}/Myf^{+}$ cell that has entered the myogenic lineage [111,113]. Interestingly, asymmetric localization of Partitioning-defective protein (Par) complexes interacting with dystrophin is another example of intrinsic regulators of asymmetric division [114,115]. In SC self-renewal, Pax7 is essential for maintenance of the muscle stem cell status, and SC survival via anti-apoptosis as demonstrated in *Pax7* knockout (KO) mice [105,107].

While many models for the study of skeletal muscle regeneration exist, the cardiotoxin (CTX)-induced injury model in mice is one of the most reproducible. CTX venom from the cobra is a polypeptide capable of inducing degeneration and subsequent

regeneration of skeletal muscle [116]. In a response comparable to the regeneration process observed in humans, the first phase involving fiber necrosis and infiltration of inflammatory response factors is observed within 2 hours of injury induced by CTX injection [61,117]. SCs then enter the activation phase followed by the proliferation period 2 to 3 days post-injury [61,117]. The differentiation phase can be histologically identified when myoblasts withdraw from the cell cycle and form small calibre, centrally-nucleated myotubes [61,117]. Finally, fusion of the myoblasts and further growth of the myofibers into regenerated muscle tissue comparable to healthy functional tissue occurs within 2 weeks of the CTX-injection [61,117]. Mature myofibers of normal sized fibers and the movement of the nuclei to the periphery are not observed until one month after CTX-injection [61,117]. The caveat to this model is the potential unknown effects of CTX on skeletal muscle molecular mechanisms [61,117].

1.4 Duchenne Muscular Dystrophy

Muscle development and regeneration are processes highly dependent on myoblast and SC differentiation and proliferation. However, dysregulation of these cellular processes is often observed in skeletal muscular dystrophies such as Duchenne muscular dystrophy (DMD).

DMD is a fatal X-linked genetic disease that is the second most commonly inherited disorder in males (affecting 1 in 3600 live male births) and leads to aggressive, severe muscle wasting in boys and young men [118,119]. It is characterized by an absence of dystrophin due to mutations in the dystrophin gene – the largest gene known in the human genome. Dystrophin is normally present all along the sarcolemma of muscle

fibers and links internal cytoskeletal elements of the myofibers to the extracellular matrix through the dystrophin-associated glycoprotein complex to maintain muscle structure and function [118,119]. In the absence of dystrophin, DMD pathology is thought to progress due to (1) mechanical stress and (2) SC dysfunction [115,120,121]. Dystrophin in healthy individuals provides strength to the sarcolemma during contractile activity [120]. Thus, the absence of dystrophin in DMD individuals puts the skeletal muscle under high mechanical stress [120]. The integrity of the sarcolemma is compromised leading to various downstream pathophysiological effects such as abnormal Ca^{2+} homeostasis and disrupted P_2X cell signalling [93,122,123]. In addition, the absence of dystrophin has also been reported to disrupt intrinsic mechanisms of SC asymmetric division such as Par-complex-dependent regulation of SC polarity leading to SC dysfunction and an accumulation of senescent SCs [115,121]. Myoblasts and SCs from animal models and DMD individuals do not effectively differentiate, fuse and proliferate in what some groups describe as SC exhaustion [124,125]. Ultimately, there is a high demand of degeneration-regeneration cycles, regenerative capacity is reduced, and myofibers rapidly undergo necrosis to be replaced with fibrotic, adipose and connective tissues, further exacerbating muscle weakness [126]. In this regard, fast-twitch fibers are preferentially affected in DMD disease [127–129].

A popular model for the study of DMD is the *mdx* mouse generated from the C57BL/10 line first discovered due to histological evidence of myopathy and elevated levels of serum creatine kinase [130]. The dystrophin-deficient phenotype arises from a nonsense point mutation (C to T transition) in exon 23 [131]. These *mdx* mice experience progressive muscle dystrophy leading to premature death [132]. Moreover, *mdx* mice display many cellular and biochemical phenotypes characteristic of early DMD

manifestation such as accumulated macrophages and skeletal muscle degeneration [133]. The caveat to this mouse model is that the severity of the clinical symptoms is minimal when compared to DMD cases [134]. For example, their lifespan is reduced by only 25% compared to 75% reduction observed in DMD patients [135]. In the two weeks after birth, *mdx* mice do not display any apparent manifestations of disease until 3-6 weeks old at which point skeletal muscles undergo rapid necrosis and mice demonstrate visible muscle weakness [135]. Afterwards, the skeletal muscles become relatively stabilized due to robust regeneration as indicated morphologically by centrally-nucleated myofibers [135]. This milder dystrophy is explained by the dystrophin deficiency being partially compensated by the upregulation of functional and structural homologs, specifically utrophin and α7-integrin in *mdx* mice [135,136]. As such, utrophin/dystrophin double knockout (*dKO*) mice are considered more relevant models of DMD [136]. The caveat with these *dKO* mice is that they are difficult to generate and maintain, and usually die prematurely in 6-20 weeks as opposed to the lifespan of up to 2 years for *mdx* mice [135,136].

Currently, there is no cure; although, various therapeutic strategies have been proposed for DMD. Firstly, the restoration of dystrophin or dystrophin-like function is the most direct therapeutic approach. To this end, various strategies exist such as gene delivery of dystrophy or utrophin, exon skipping and mutation suppression to correct the faulty parts of the dystrophin gene, and *in vivo* and post-natal genome editing via CRISPR/Cas9 [137–141]. Other approaches seek to improve the secondary pathological effects downstream of the dystrophin deficiency in order to increase muscle mass, strength and force [142]. Examples include pharmacological approaches such as steroid treatment, cell and stem cell therapy such as those involving myoblasts and SCs, and

pharmacological treatments like WNT7a that seek to augment regeneration [79,121,142–145]. Combinatorial therapies involving the transplantation of genetically-corrected cells is also often discussed [142,146]. Overall, many of the current strategies to treat DMD do not take SCs into consideration. For example, gene delivery methods of treating DMD seen in the literature often use the adeno-associated vector system; however, this vector system is not very efficient at targeting SCs which may hinder their therapeutic capacity [147]. Moving forward with the emerging evidence that DMD is a stem cell disease in addition to one of myofiber fragility, the development of novel therapeutic strategies should focus on restoring SC function in addition to ameliorating the secondary effects of muscle wasting by augmenting regeneration [121,144,148]. Given that previous work from our laboratory has demonstrated important roles for Panx1 and Panx3 in regulating myoblast differentiation and proliferation [14], a better understanding of Panx1 and Panx3 channel function in muscle development, regeneration, and DMD, as well as their function in SCs, may provide new insight into the pathology of DMD in addition to novel therapeutic strategies for this disease.

1.5 Pannexins in Skeletal Muscle

Panx1 was first detected in human and mouse skeletal muscle at the mRNA level in 2004 [3]. However, it was not until 2012 that Panx1 in skeletal muscle started to be investigated. In rodent adult skeletal muscle fibers, Panx1 protein has been localized to the sarcolemma and the T-tubules of rodent skeletal muscle fibers [149,150]. Panx1 channels have been shown to be involved in skeletal muscle contraction [150], skeletal muscle

plasticity [27,149], excitation-transcription coupling [151,152], myogenic commitment [153], and myoblast differentiation [14].

Upon electrical stimulation, Panx1 channels release ATP and uptake glucose, suggesting its involvement as channel proteins in the potentiation of muscle contraction [150]. To increase the force of contraction after repetitive twitches, extracellular ATP is necessary for this potentiation of muscle contraction especially in fast-twitch muscles [150,154]. ATP release after stimulation from channels like Panx1 can activate P_2Y_1 receptors to trigger downstream signalling effects that increase Ca^{2+} release from intracellular stores - another crucial element of the potentiation response [150]. In contrast, slow-twitch muscles rely on accumulation of cytoplasmic free Ca^{2+} from extracellular stores to potentiate muscles via purinergic ionotropic P_2X_4 receptors, which are highly expressed in this muscle type [150,154]. When skeletal muscle myotubes were isolated in culture, ATP release during electrical stimulation was inhibited upon addition of Panx1 channel blockers; however, the Panx1 channel blockers had no effect in the adult soleus muscle nor in *Panx1* KO mice [150]. Similarly, *Panx1* KO mice did not demonstrate muscle potentiation until the exogenous addition of ATP, confirming that Panx1 channels are necessary for the potentiation response by releasing ATP [27,149,150].

Another physiologically important process in skeletal muscle is plasticity, which involves remodelling structure and performance output to meet functional demand [155,156]. Indeed, fast-twitch fibers that have been mechanically stimulated at a specific frequency demonstrate transcriptional changes related to fast-to-slow type transition. Panx1 channels have been involved in this transition by releasing ATP, which activates the IP_3-dependent intracellular Ca^{2+} signal in order to affect transcriptional activity [27]. This ATP-

induced Ca^{2+} signal was inhibited by Panx1 channel blockers [151]. As such, ATP release by Panx1 to stimulate purinergic receptors and elicit an intracellular Ca^{2+} response may regulate not only skeletal muscle potentiation, but also plasticity. Indeed, the ATP release mediated by Panx1 channels after electrical stimulation was shown to play a key role in transcription of the slow-type troponin (TnI) gene [149], a signature of the fast-to-slow muscle fiber phenotype transition [157].

In addition to their role in the potentiation of contraction and skeletal muscle plasticity, it has been proposed that electrical stimulation of skeletal muscle cells triggered the production of reactive oxygen species (ROS) in part through Panx1 channels and purinergic P_2Y_1 activity [158]. It was demonstrated that the increase in ROS production induced by electrical stimulation could be blocked by carbenoxolone [158]. This effect was mimicked by exogenous ATP suggesting that ATP released via Panx1 channels during electrical stimulation is necessary to increase ROS production during depolarization of skeletal muscle fibers [158]. Furthermore, absence of Panx1 (in Panx1 KO mice) also prevented an increase in ROS induced by skeletal muscle denervation [159]. Altogether these data suggest that Panx1 channels are relevant to adult skeletal muscle health by regulating the potentiation of the contraction response, muscle plasticity that allows adaptation to demand, and the oxidative state during exercise or upon electrical stimuli.

As mentioned previously, muscle development and regeneration involve myogenic commitment, proliferation, and differentiation of myoblasts and SCs. Early work revealed that blocking of Panx1 channels using β-glycyrrhetinic acid prevented the expression of differentiation markers like myogenin [24]. Coordination of ATP release with

Ca^{2+} signalling necessary for myoblast differentiation through the action of P_2X receptors has been suggested using C_2C_{12} cells prior to the identification of Panx as ATP channels [160]. Our laboratory has recently shown that Panx1 and Panx3, but not Panx2 channels, are co-expressed in the skeletal muscle of both humans and rodents [14]. However, it was later suggested that a novel commercial monoclonal antibody (clone N121A/1) may detect Panx2 protein in murine skeletal muscle tissue [11]. Findings from my laboratory recently revealed that PANX1 channels promote the differentiation and fusion of human primary myoblasts [14]. Interestingly, the development of skeletal muscle from fetal to adult tissue corresponds to a transition from high proliferative activity of myoblasts to differentiated myofibers in which the contribution by cell proliferation decreases. We found that the higher MM species of PANX1 (~50 kDa) is the main form present in both fetal and adult human skeletal muscle. However, it decreases in the adult tissue whereas the lower MM forms, known as Gly0 and Gly1 [23] become more abundant [14]. *In vitro,* a significant increase in PANX1 levels during the differentiation of myoblasts was observed [14]. Furthermore, over-expression of PANX1 promoted myoblast differentiation and fusion, while these processes were inhibited by the PANX1 channel blockers probenecid and carbenoxolone [14]. As for PANX3, the results suggested that its low MM species (~37-50 kDa) is involved in maintaining the differentiated and non-proliferative state of myoblasts, while its ~70 kDa immunoreactive species may be required to keep the undifferentiated myoblasts in a proliferative state. The low MM species of PANX3 was detected at low levels in fetal skeletal muscle tissue but increased in adult skeletal muscle [14]. Over-expression of the low MM species of PANX3 induced human primary myoblasts differentiation while inhibiting their proliferation [14]. In contrast, its ~70 kDa

immunoreactive species was highly expressed in fetal skeletal muscle tissue and in proliferative human primary myoblasts [14]. However, its levels drastically diminished below detectable levels in adult tissue and upon myoblast differentiation [14]. shRNA knockdown of the ~70 kDa immunoreactive species of PANX3 significantly inhibited myoblast proliferation without triggering cell differentiation [14]. A subsequent study involving reserve cells (RCs), which are a subpopulation of the murine skeletal muscle C_2C_{12} cell line that have many characteristics similar to SCs by reversibly exiting the cell cycle post-differentiation and entering a quiescent-like state, showed that Panx1 channels induced myogenic commitment [153]. Panx1 channels, likely through the release of ATP, along with the activation of P_2X receptors are required for the myogenic commitment of RCs [153]. Indeed, exogenous ATP induced RC myogenic commitment, as observed by the increase in MyoD expression. On the other hand, Panx1 channel KO or P_2 channel inhibition blocked myogenic commitment [153]. Taken together, these data raise the possibility that Panx1/PANX1 and Panx3/PANX3 channels play a crucial role in muscle development and regeneration by regulating the proliferation and differentiation of both myoblasts and SCs.

Finally, recent studies suggest that Panx1 channels may play a role in skeletal muscle dystrophy. *Valladares et al.* reported that skeletal muscle triads from *mdx* mice had higher levels of Panx1 and P_2Y_2 receptors, which may cause the increase in ATP release observed only in fibers at basal condition [161]. This increase in ATP release, together with the activation of pro-apoptotic pathways, was proposed to contribute to muscular dystrophy [161]. In isolated primary muscle cells, cell lines and *in vivo* dystrophic muscle from the *mdx* mouse model, significant P_2X_7 receptor abnormalities have been

reported. For example, up-regulated P_2X_7 mRNA and protein expression has been associated to increased responsiveness of cytoplasmic Ca^{2+} and extracellular signal-regulated kinase (ERK) 1/2 phosphorylation associated to purinergic activation [162]. Though Panx1 transcripts were present, this study reported no P_2X_7 interactions with Panx1 [162]. Interestingly, Panx1 has been shown to interact with dystrophin, along with other proteins of the excitation-transcription (E-T) coupling machinery: voltage sensor dihydropyridine receptor (DHPR, $Ca_v1.1$), and P_2Y_2 receptors [152]. In *mdx* skeletal muscle triads, Panx1 expression is also increased; however, DHPR expression is decreased suggesting a disruption of the E-T coupling complex in the absence of dystrophin [152]. Overall, altered levels and channel activity of Panx1 may play a role in muscular dystrophy, while the role of Panx3 remains to be examined. Indeed, there is very little information about Panx3 in skeletal muscle health and disease. In one report, Panx3 may be involved in monocyte attraction towards mouse skeletal muscle in the context of inflammation and obesity [163]. Moreover, phenotypic analysis of long bones in Panx3 KO mice revealed relatively larger prominences where skeletal muscle attachment occurs, suggesting increased strain [164].

1.6 Hypothesis and Objectives

As mentioned above, our laboratory has recently found that PANX1 and PANX3 levels are highly regulated during myoblast differentiation and, importantly, has identified PANX1 and PANX3 channels as novel regulators of skeletal muscle myoblast differentiation and proliferation. Given that these cellular processes, together with SCs, are crucial for proper myogenesis, **I hypothesize that Panx1 and Panx3 are involved in**

muscle development, regeneration and dystrophy. In addition to promoting the differentiation of myoblasts, I hypothesize that PANX1 channels also regulate the differentiation and proliferation of SCs. My first objective was to determine whether Panx1 and Panx3 are differentially expressed in fast- vs. slow-twitch muscles and in male vs. female mice. My second objective was to determine whether Panx1 and Panx3 levels are regulated during *in vivo* processes dependent on myoblast and SC differentiation and proliferation such as muscle development, regeneration, and muscular dystrophy. Finally, my last objective was to determine whether PANX1 levels are modulated during SC differentiation and whether PANX1 channels regulate SC differentiation and proliferation. A better understanding of Panx1 and Panx3 regulation in muscle development, regeneration, and dystrophy, as well as their function in SCs, may provide new information on their role in skeletal muscle health and disease.

2.0 MATERIALS AND METHODS

2.1 Primary Cells, Cell Lines, and Culture Conditions

Primary Human Skeletal Muscle Satellite Cells (human SCs) taken from human muscle of the pectoral girdle were propagated as specified by the supplier (ScienCell, Carlsbad, CA) on Matrigel-coated (Corning, Tewksbury, MA) plates and maintained in Skeletal Muscle Cell Medium (SkMCM; ScienCell). Primary Human Skeletal Muscle Myoblasts (HSMM) were obtained from Lonza (Walkersville, MD), and propagated, maintained and differentiated as previously described [14]. Human embryonic kidney HEK 293T cells were from ATCC (Manassas, VA) and maintained in DMEM + 10% FBS.

2.2 Plasmids and Transfections

Untagged Panx1 and Panx3 expression constructs have been previously described [4,23]. HEK 293T cells were transfected using Lipofectamine 2000 (Life Technologies, Carlsbad, CA) and used as positive controls for pannexin expression.

2.3 Mice

All experimental protocols were approved by the University of Ottawa Institutional Animal Care Committee and were in accordance with the Canadian Council of Animal Care guidelines. For experiments comparing different skeletal muscle types, 4-week-old FVB/N mice (Charles River Laboratories) were used. Mice were euthanized and the *tibialis anterior* (TA), *extensor digitorum longus* (EDL), *soleus* (SOL) and diaphragm (DPH) were harvested and immediately frozen in liquid nitrogen and then stored at -80 C until use or embedded in Tissue-Tek OCT Compound (Sakura Finetek,

Torrance, USA), frozen in melting isopentane pre-cooled with liquid nitrogen and then stored at -80 °C until use.

For developmental time course experiments, skeletal muscles from FVB/N mice were used. Skeletal muscles from mouse embryos were harvested at E14.5 and E18.5. Skeletal muscles from newborns PN1, as well as from 4-week-old and 12-week-old mice were also recovered. Due to the small size of limbs at embryonic (E14.5 and E18.5) and newborn (PN1) ages, the whole muscle mass of the leg was used, while the TA muscles from 4-week-old and 12-week-old mice were utilized. After being harvested, muscles were immediately frozen in liquid nitrogen and then stored at -80 °C until use.

For degeneration/regeneration experiments, 25 µl of 10^{-5} M cardiotoxin (Latoxan, Rosans, France) were injected by John Lunde from Dr. Bernard Jasmin's laboratory into the tibialis anterior (TA) muscle of 5- to 6 week-old FVB/N mice to induce muscle degeneration and regeneration as previously described [165–167]. At different time points after injection, mice were euthanized, TA muscles were harvested, frozen in liquid nitrogen or embedded in Tissue-Tek OCT Compound, and stored at -80 °C until further analysis. Contralateral, saline-injected TA muscles were used as controls.

For experiments with dystrophic mice, 4-week-old C57BL/10ScSn-Dmd^{mdx}/J (*mdx* mice) dystrophin-deficient mice (The Jackson Laboratory, Bar Harbor, ME) or 8-week-old utrophin/dystrophin double knockout (Utrn^{tm1Ked}Dmd^{mdx}/J; *dKO*) mice, bred as previously described [168], were compared to 4- and 8-week-old parent line C57BL/10ScSnJ mice (The Jackson Laboratory), respectively. Mice were euthanized and the *tibialis anterior* (TA), *extensor digitorum longus* (EDL), *soleus* (SOL), and diaphragm (DPH) were harvested and immediately frozen in liquid nitrogen and then

stored at -80 C until use or embedded in Tissue-Tek OCT Compound, frozen in melting isopentane pre-cooled with liquid nitrogen and then stored at -80 °C until use.

2.4 RNA Extraction, Reverse Transcription, and Quantitative PCR Analysis

Skeletal muscle tissues total RNA was extracted using RNAzol RT as per manufacturer's instructions (Sigma-Aldrich, Oakville, ON). Reverse transcription was performed using High Capacity cDNA Reverse Transcription Kit (Thermo Scientific, Waltham, MA) according to the manufacturers' protocols. The synthesized cDNA was used as the template for quantitative PCR using iQ™ SYBR® Green Supermix kit (BioRad) on Mastercycler ep *realplex* (Eppendorf, Mississaugua, ON, Canada) real-time PCR system with gene specific primers for mouse *Panx1* (Mm_Panx1_1_SG; Qiagen, Hilden, Germany) and mouse *Panx3* (Mm_Panx3_1_SG; Qiagen). Expression levels were normalized to the geometric mean of three internal control genes: *Gapdh*, *Ppia*, and *Rpl13a*. Specific primers for mouse Gapdh, Ppia, and Rpl13a were from the Mouse Housekeeping Gene Primer Set purchased from Real Time Primers (Elkins Park, PA).

2.5 Tissue Homogenization, Cell Lysis, and Western Blot Analysis

Skeletal muscle tissues were homogenized in 1% Triton X-100, 150 mM NaCl, 10 mM Tris, 1 mM EDTA, 1 mM EGTA, 0.5% NP-40, phosphatase inhibitor phosSTOP (Sigma, Oakville, ON), and proteinase inhibitor mini-EDTA tablet (Roche-Applied Science, Laval, QC) using the Omni Bead Ruptor with 2.38 mm stainless steel beads. HSkMSC, HSMM and HEK293T cell lysates were obtained as previously described [14,22].

After separation by SDS-PAGE, proteins were transferred to PVDF membranes and immunoblotted with anti-Panx1 (clone mPanx1B_34, 1:1000) [4], anti-PANX1 (1:1000; Sigma, Oakville, ON, Canada), anti-Panx3 (clone mPanx3_28, 1:1000) [4], and anti-myosin heavy chain (1:1000; R&D Systems, Minneapolis, MN). The hybridoma, monoclonal Pax7 antibody concentrate was obtained from the Developmental Studies Hybridoma Bank, created by the NICHD of the NIH and maintained at The University of Iowa, Department of Biology, Iowa City, IA 52242. Secondary antibodies conjugated to Alexa 680 (Invitrogen) or infrared fluorescent dye IRDye 800 (Rockland Immunochemicals, Gilbertsville, PA) were used (1:5000), and immunoblots were quantified using the Odyssey infrared-imaging system (Licor). The membranes were reprobed for either ribosomal protein S6 (RPS6) (clone C-8, 1:1000; Santa Cruz, Dallas, TX) or glyceraldehyde-3-phosphate dehydrogenase (GAPDH) (1:5000; Advanced ImmunoChemical Inc, Long Beach, CA) for normalization of protein loading. Protein standards are depicted in kDa. Lysates from HEK 293T cells over-expressing either Panx1 or Panx3 were used as positive controls.

2.6 Immunofluorescence Analysis of Tissues and Cells

Skeletal muscle cryosections (10µm) were prepared then fixed in prechilled 80% methanol + 20% acetone for 10 minutes at -20°C, followed by blocking and permeabilizing in 3% BSA +0.1% Triton X-100 (in PBS) for 1 hour at room temperature. Cryosections were stained overnight at 4 °C using the following primary antibodies diluted in 1% BSA + 0.1% Tween-20 + 0.01% SDS (in PBS): Panx1 (1:50), Panx3 (1:50) [4,23], caveolin-1 (Cav-1) (1:50; Santa Cruz, Dallas, TX), and laminin (1:1000; Sigma).

Appropriate antibodies conjugated to Alexa-Fluor 488 or 594 (Life Technologies) diluted in 1% BSA were used for secondary detection at room temperature. Hoechst 33342 (Molecular Probes, Eugene, OR) was utilized to stain the nuclei and the tissue section slides were then mounted using Fluoromount (SouthernBiotech, Birmingham, AL). For hematoxylin and eosin staining, cryosections were washed in 95% ethanol followed by 70% ethanol for 2 minutes per wash. They were stained in hematoxylin for 30 seconds, then destained in 1% HCl acid (in ethanol) followed by treatment in 0.1% sodium bicarbonate for 1 minute. They were washed again in 70% and 90% ethanol for 1 minute per wash before the eosin staining for 30 seconds. To dehydrate cryosections, they were treated with increasing concentration of ethanol from 70-100% ethanol followed by xylene and mounting with Permount.

Human SCs were fixed in 3.7% paraformaldehyde for 5 minutes at room temperature. Cells were permeabilized in 0.5% Triton X-100 + 0.1M glycine (in PBS) for 15 minutes and blocked in 5% horse serum + 2% BSA + 0.1% Triton X-100 (in PBS) for 2 hours at room temperature. Cells were stained overnight at 4 °C using the following antibodies diluted in blocking buffer: PANX1 (1:1000; Sigma, Oakville, ON, Canada), Pax7 (concentrate, DSHB), MyoD (clone M-318, 1:50, Santa Cruz), myogenin (MYOG) (clone F5D, 1:50, Santa Cruz), and myosin heavy chain (clone MF20, 1:100, R&D Systems, Minneapolis, MN). Appropriate secondary antibodies conjugated to Alexa-Fluor 488, 594 or 647 (Life Technologies) were used. Cells were mounted using Fluoromount-G containing DAPI (Southern Biotech, Birmingham, AL). High-resolution images were acquired using our Olympus Fluoview FV1000 confocal microscope.

2.7 Differentiation Assay

To induce differentiation, human SCs were switched to DMEM + 2% horse serum + 1% penicillin/streptomycin. For Panx channel inhibition experiments, pharmacological compounds were added to a final concentration of 1 mM probenecid or 100 µM carbenoxolone for 24 hours. Cells were fixed for immunofluorescent staining to quantify the percentage of Pax7/MyoD-, myogenin (MyoG-), and MHC-positive cells and fusion index. The differentiation index was calculated as the percentage of MHC-positive cells above total nuclei and the fusion index as the percentage of MHC-positive cells above total nuclei. The proportions of MHC-positive cells containing 2-4, 5-9, and 10-25+ over total nuclei were also compared [169]. To compare PANX1 levels in MyoD- and MHC-negative cells compared to MyoD- and MHC-positive cells at D0 and D6, the PANX1 labelling was quantified using Image J (U.S. National Institute of Health, MD) by defining a region of interest around a PANX1-labelled cell and measuring the average intensity per unit squared, denoted as relative units [170]. Ten cells of each expression profile (MyoD- and MHC-negative cells, and MyoD- and MHC-positive cells) were arbitrarily chosen from one independent experiment. Measurements were taken from at least three independent experiments.

2.8 Proliferation Assays

Human SCs were plated in 24-well plates at 30,000 cells per well and incubated with 10µM 5-bromo-2-deoxyuridine (BrdU) (Sigma-Aldrich) at 37 °C for 2 hours. Cells were fixed in 3.7% paraformaldehyde for 20 minutes followed by blocking and permeabilization in 2% BSA + 0.1% Triton X-100 (in PBS) for 1 hour. Cells were treated

with 2N HCl for 20 minutes at room temperature to denature the DNA followed by immunofluorescent staining with BrdU antibody (clone ZBU30, 1:100, Life Technologies) as described above. BrdU staining was visualized with Life Technologies EVOS FL Auto Cell Imagine System. The level of BrdU incoporation correlating to human SC proliferation was quantified by counting the number of BrdU-positive cells over the total number of nuclei in a field for a total of at least 10 fields randomly chosen per independent experiment. For BrdU-ELISA assays, Cell Proliferation ELISA, BrdU (colorimetric) (Roche Life Science) was used according to manufacturer's protocol with a BrdU pulse time of 2 hours. Absorbance values were read according to manufacturer's protocol using Synergy HTX Multi-mode Reader (Biotek, Winooski, VT). For Panx channel inhibition experiments, probenecid or carbenoxolone was added at a final concentration of 1mM or 100uM, respectively, for 24 hours. Measurements from at least three independent experiments were taken.

2.9 Statistical Analysis

The data were analyzed for statistical significance using unpaired two-tailed Student's *t*-tests and analysis of variance (ANOVA) followed by Tukey's post-hoc tests, as appropriate. Statistical significance was accepted at $P < 0.05$.

3.0 RESULTS

3.1 Panx1 and Panx3 are differentially expressed and localized in distinct skeletal muscle types

Skeletal muscles are composed of slow- and fast-twitch muscle fibers. Slow-twitch fibers are more resistant to fatigue than their counterpart, partly because of their mitochondrial volume and higher activity of oxidative enzymes [171–173]. In addition, the contractile response time course of slow-twitch fibers, as the name implies, is substantially slower than that of fast-twitch fibers [173]. In order to characterize Panx1 and Panx3 expression in skeletal muscle and get insight into their potential functions in healthy and diseased skeletal muscle *in vivo*, we compared their expression levels and localization in muscles that are predominantly fast-twitch (TA and EDL) and slow-twitch (SOL) muscles in male and female mice. Our qPCR analysis revealed that *Panx1* transcript levels are significantly increased in SOL compared to those of TA and EDL muscles, but were the same between male and female muscles (**Fig. 1A**). As expected, various molecular mass (MM) species of Panx1 were detected by Western blot in skeletal muscles (**Fig. 1B**), likely reflecting different glycosylation statuses [4]. In accordance with our qPCR data, all Panx1 MM species calculated together showed levels significantly enhanced in SOL compared to TA and EDL muscles (**Fig. 1C**). Muscle cross-sections correspondingly indicated increased Panx1 staining (green) in slow-twitch muscles compared to fast-twitch muscles. Laminin (red) was labeled to depict individual muscle fibers. Panx1 was detected as small punctate structures throughout the myofibers with areas of the cell surface more heavily labeled (**Fig. 1D**).

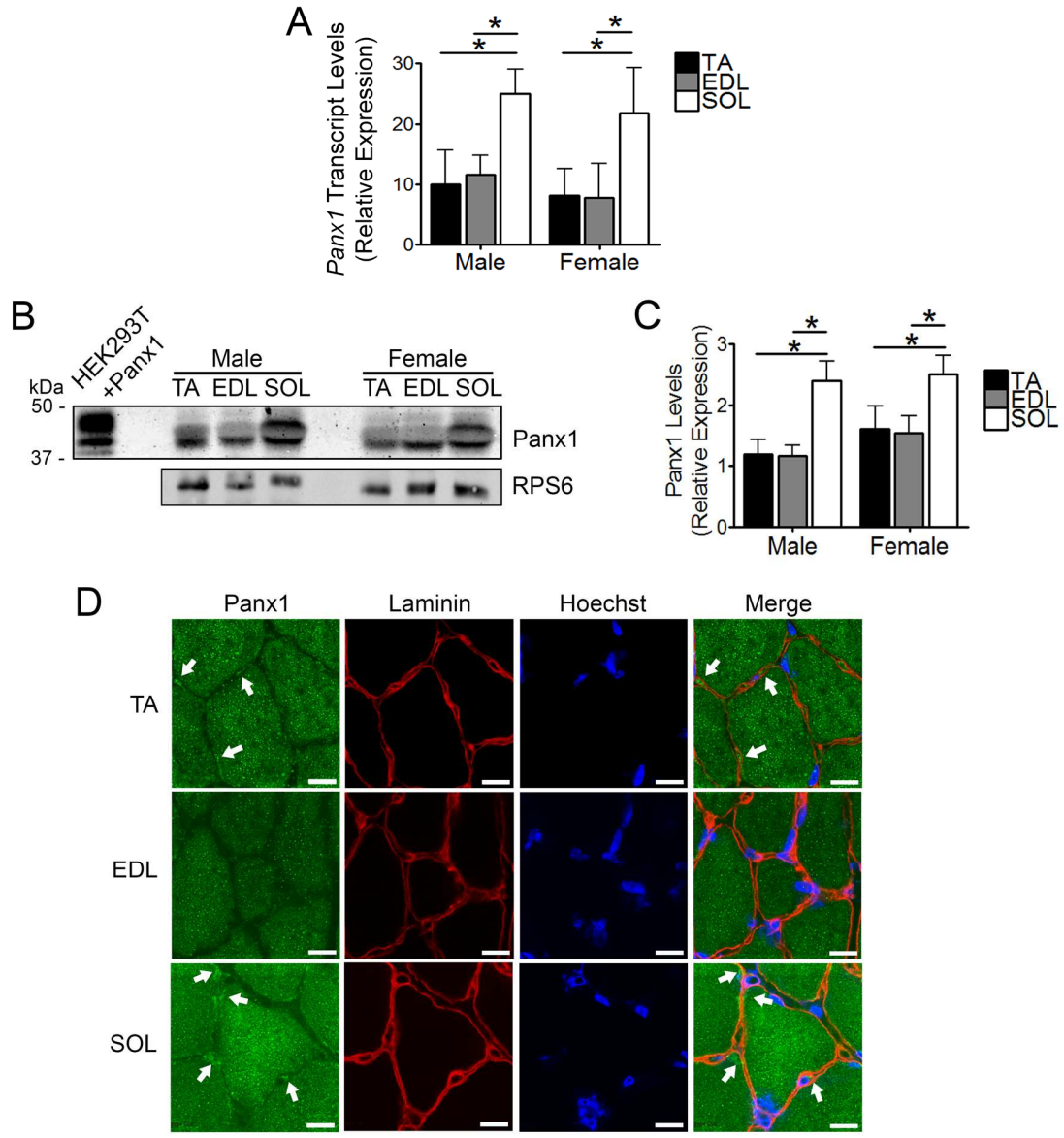

Figure 1. Panx1 is differentially expressed and localized between TA, EDL, and SOL skeletal muscles. (A) Relative expression of *Panx1* transcripts were measured in fast-twitch (TA, EDL) and slow-twitch (SOL) skeletal muscles from male (n=4) and female (n=4) mice and showed higher expression of *Panx1* in SOL compared to TA and EDL in both males and females. Data are mean ± SD, *p≤0.05. Protein levels of Panx1 in male and female TA, EDL, and SOL were analyzed by Western blotting **(B)** and quantified **(C)**. Various molecular weights species of Panx1 were detected. Panx1 protein levels were higher in SOL compared to TA and EDL in both males and females. HEK 293T cells transfected with Panx1 were utilized as a positive control, while ribosomal protein S6 (RPS6) was used as a loading control. Data are mean ± SD, *p≤0.05 (n=4). **(D)** Cross-sections of TA, EDL, and SOL muscles from male mice were labeled for Panx1 (green) and laminin (red). Representative images are shown. Panx1 was detected

as a punctate stain throughout the myofiber with areas of the cell surface more heavily labelled (white arrows). Blue = nuclei, bars = 10µm.

In contrast, *Panx3* transcript levels were significantly decreased in SOL compared to EDL muscles (**Fig. 2A**). Male and female muscles expressed similar *Panx3* expression levels (**Fig. 2A**). Upon Western blot analysis, Panx3 antibody detected ~35-40 kDa bands corresponding to its expected molecular weight, as well as its ~70 kDa immunoreactive species (**Fig. 2B**) [4]. Interestingly, the levels of the low MM species of Panx3 were significantly diminished in SOL compared to EDL muscles, while the levels of the ~70 kDa immunoreactive species of Panx3 remained similar between muscle types (**Fig. 2C-D**). No significant difference in Panx3 levels was observed between male and female muscles (**Fig. 2C-D**). In keeping with our Western blot data, cross-section staining showed a decrease in Panx3 labeling in SOL muscle (**Fig. 2E**). Panx3 was detected as a punctate staining throughout the myofibers with increased labeling localized at and in proximity to the cell surface of the muscle fibers (**Fig. 2E**). This staining likely represents the low MM species of Panx3 as the antibody used here is believed to be incapable of detecting the ~70 kDa immunoreactive species by immunofluorescent staining [4]. Thus, Panx1 and Panx3 show differential expression and localization in the various skeletal muscle types, which may reflect fiber type-specific and membrane- versus cytoplasmic-specific functions.

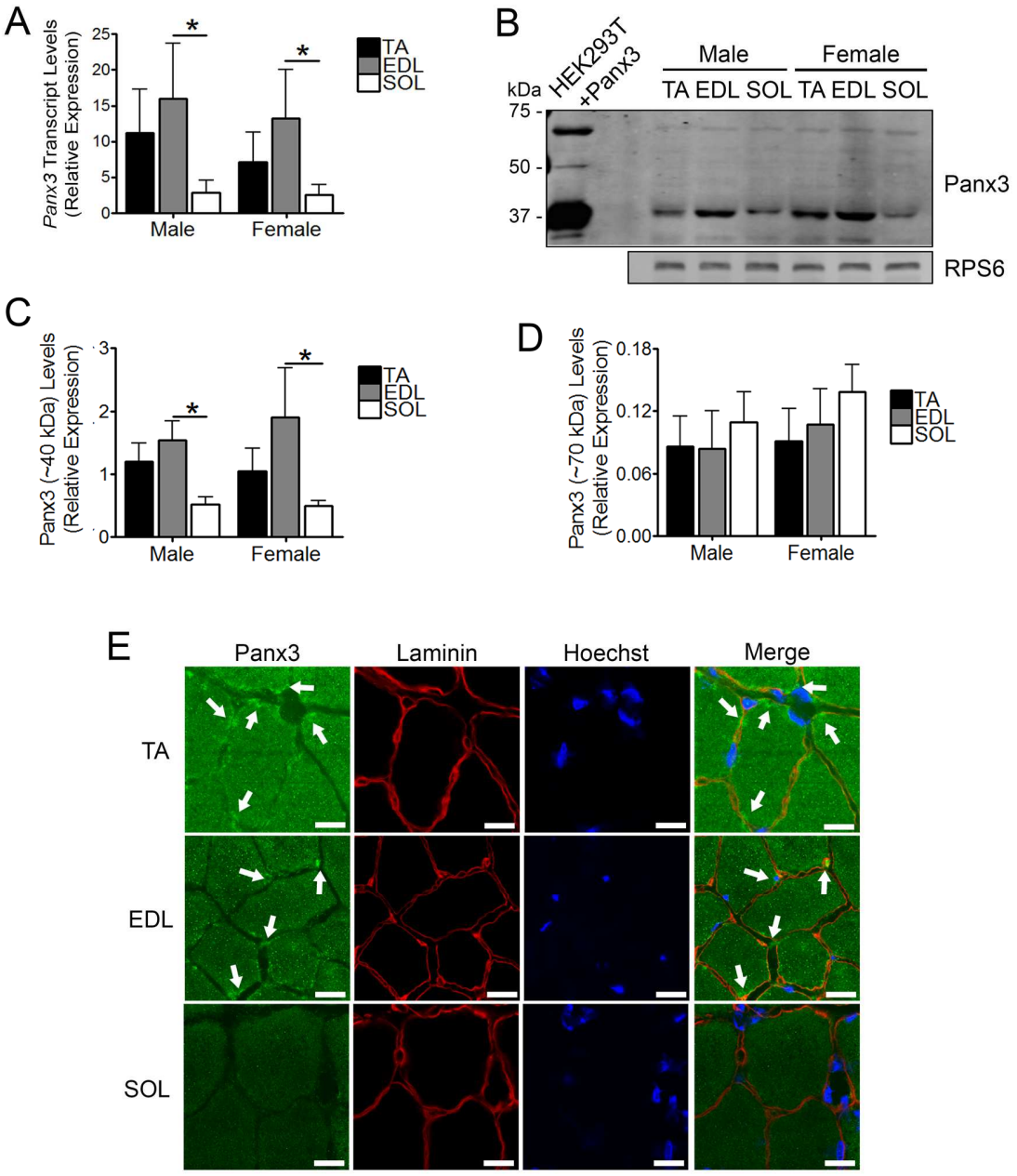

Figure 2. Panx3 is differentially expressed and localized between TA, EDL, and SOL skeletal muscles. (A) Relative expression of *Panx3* transcripts was measured in fast-twitch (TA, EDL) and slow-twitch (SOL) skeletal muscles from male (n=4) and female (n=4) mice and showed lower expression of *Panx3* in SOL compared to EDL in both males and females. Data are mean ± SD, *p<0.05. Protein levels of Panx3 in male and female TA, EDL, and SOL were analyzed by Western blotting **(B)** and quantified **(C-D)**. Various molecular weights species of Panx3 were detected. The levels of the low molecular weight species (~40 kDa) of Panx3 were significantly lower in SOL compared to EDL in both males and females **(B-C)**, while there was no significant difference in the levels of its ~70 kDa immunoreactive species **(B-D)**. HEK 293T cells transfected with

Panx3 were utilized as a positive control, while ribosomal protein S6 (RPS6) was used as a loading control. Data are mean ± SD, *p<0.05 (n=4). **(D)** Cross-sections of TA, EDL, and SOL muscles from male mice were labeled for Panx3 (green) and laminin (red). Representative images are shown. Panx3 was detected as a punctate stain throughout the myofiber with areas of the cell surface more heavily labeled (white arrows). Blue = nuclei, bars = 10µm.

3.2 Panx1 and Panx3 levels are regulated during skeletal muscle development

Having reported that PANX1 and PANX3 levels are differentially expressed in fetal and adult human skeletal muscle tissue [14] and to better understand the roles of Panx1 and Panx3 in skeletal muscle *in vivo*, we examined their expression pattern during mouse muscle development. To this end, we used skeletal muscles obtained at various stages of development: embryonic (E14.5 and E18.5 fetuses); newborn (postnatal day 1 (PN1) pups); juvenile (4-week-old mice); and adult (12-week-old mice). Due to the small size of the limbs of mouse embryos, the whole muscle mass of the leg was used for E14.5 and E18.5 fetuses, as well as newborn (PN1) mice. For juvenile and adult mice, TA muscles were utilized. Our Western blot analysis and its quantification revealed that Panx1 levels increase during muscle development beginning at embryonic day 18.5 through to the juvenile stage (**Fig. 3A-B**). As for Panx3, our Western blot showed that its ~70 kDa immunoreactive species is mainly expressed in skeletal muscles from embryonic and newborn mice (**Fig. 3C**). On the other hand, the levels of the low MM species of Panx3 remained relatively constant throughout the development time course examined (**Fig. 3C-D**). As levels of the ~70 kDa immunoreactive species of Panx3 become very low or below detectable levels in juvenile and adult skeletal muscles, its low MM isoform became the prominent Panx3 species expressed in juvenile and adult skeletal muscles (**Fig. 3C-E**). Altogether, these results clearly indicate that Panx1 and Panx3 levels are

differentially regulated during muscle development suggesting distinct functions during this process.

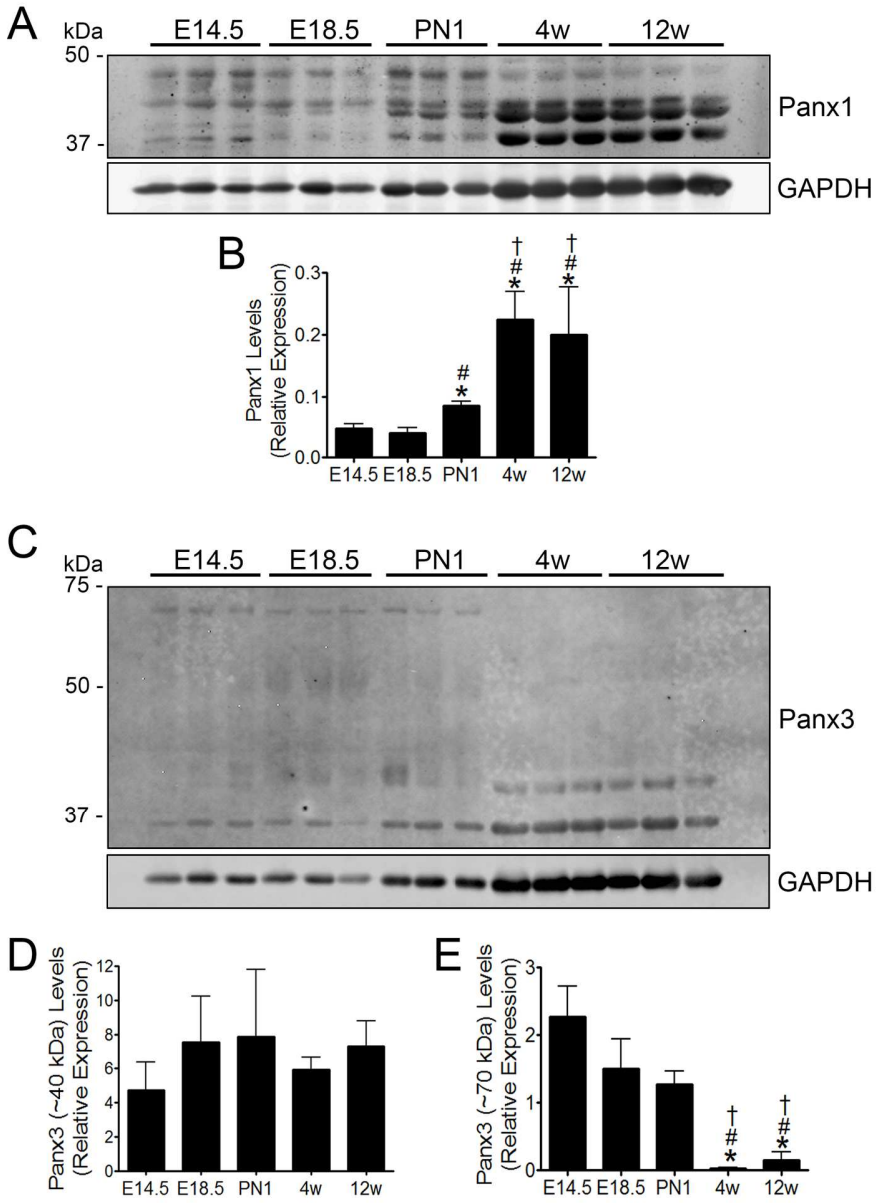

Figure 3. Panx1 and Panx3 levels are regulated during skeletal muscle development. Panx1 and Panx3 protein levels were analyzed by Western blots in murine skeletal muscle at various stages of development: embryonal (E15.4 and 18.5), newborn (postnatal day 1 (PN1)), juvenile (4-week-old (4w)), and adult (12-week-old (12w)). GAPDH was used as a loading control. Panx1 levels significantly increased from embryonic to post-natal to adult ages **(A-B)**. As for Panx3, the levels of its low molecular weight species (~35-40 kDa) remained similar throughout development (**C-D)**. However,

the levels of its ~70kDa immunoreactive species significantly decreased from the embryonic/newborn stages compared to that of the juvenile and adult mice **(C-E)**. Data are mean ± SD, *p≤0.05 compared to E14.5; # p≤0.05 compared to E18.5; † p≤0.05 compared to PN1 (n=3).

3.3 Panx1 and Panx3 are expressed in human and mouse skeletal muscle SCs

Muscle development and regeneration involve the coordination of proliferation and differentiation of myoblasts and SCs [59]. Having shown that human primary myoblasts mainly express PANX1, we next wanted to determine whether human primary skeletal muscle SCs (human SC) also express PANX1 and/or PANX3. Similar to myoblasts, various MM species of PANX1 were detected in human SC lysate (**Fig. 4A**). While the low MM species of PANX3 (~40 kDa) were detected, its ~70 kDa immunoreactive species was the most prominent (**Fig. 4A**). As expected, these cells express the SC marker PAX7 [104,105,174] but not Myosin Heavy Chain (MHC), a typical marker of terminally differentiated muscle cells (**Fig. 4A**). Using mouse skeletal muscle tissue sections, we demonstrate positive Panx1 and Panx3 staining in SCs, which were identified using anti-Caveolin 1 (Cav-1) antibody (**Fig. 4B**). Based on these results, we thus report for the first time that Panx1 and Panx3 are co-expressed in both human and mouse skeletal muscle SCs.

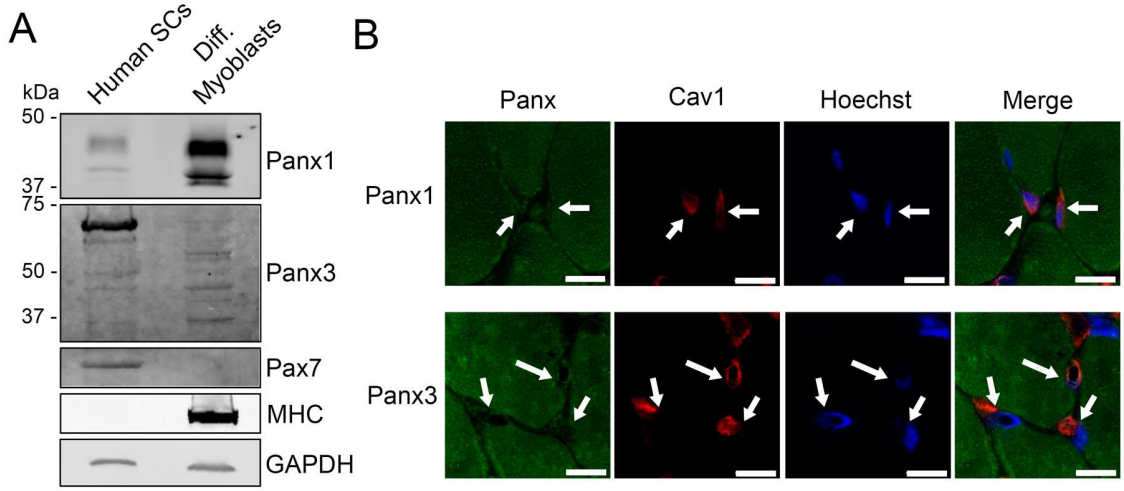

Figure 4. Panx1/PANX1 and Panx3/PANX3 are expressed in mouse and human satellite cells. (A) PANX1 and PANX3 proteins were detected by Western blot in human skeletal muscle satellite cells (Human SCs) compared to human primary skeletal muscle myoblasts that have been differentiated for 6 days (Diff. Myoblasts). Paired box protein 7 (Pax7) was used as a satellite cell marker, while myosin heavy chain (MHC) was utilized as marker of differentiated muscle cells. GAPDH was used as a loading control. **(B)** Cross-sections of murine skeletal muscle were co-labeled for Panx (Panx1 or Panx3; green) and the mouse satellite cell marker caveolin-1 (Cav1; red) **(B)**. Representative images are shown. Both Panx1 and Panx3 were detected in Cav-1-positive satellite cells (arrows). Blue = nuclei, bars = 10µm.

3.4 Panx1 and Panx3 levels are regulated during skeletal muscle regeneration

Given that SCs are the main players involved in skeletal muscle regeneration [175], and that our data indicate that Panx1 and Panx3 are expressed in these cells, we next examined whether Panx1 and Panx3 levels are modulated during skeletal muscle regeneration *in vivo*. To this end, cardiotoxin (CTX) was injected in the TA muscle of adult mice to induce severe myonecrosis and subsequent muscle regeneration [61,166,167,176,177]. Western blots were performed using TA homogenates obtained 2, 4, 7 and 14 days after CTX injection. We first measured Panx1 protein expression and observed a drastic decrease at day 2 post-injury compared to saline controls (**Fig. 5A-B**). Panx1 protein levels gradually returned to control levels 14 days post-injury when muscle fibers

are fully regenerated (**Fig. 5A-B**). To assess whether Panx1 localization was altered during skeletal muscle regeneration, TA sections at day 4 post-CTX injection were immunolabelled for Panx1 and compared to saline controls. While Panx1 staining was present throughout the myofibers with increased punctate staining in areas near the cell surface, and was consistent between CTX-treated and control TA sections, there was a general decrease in Panx1 labeling throughout the CTX-injected muscles (**Fig. 5C**).

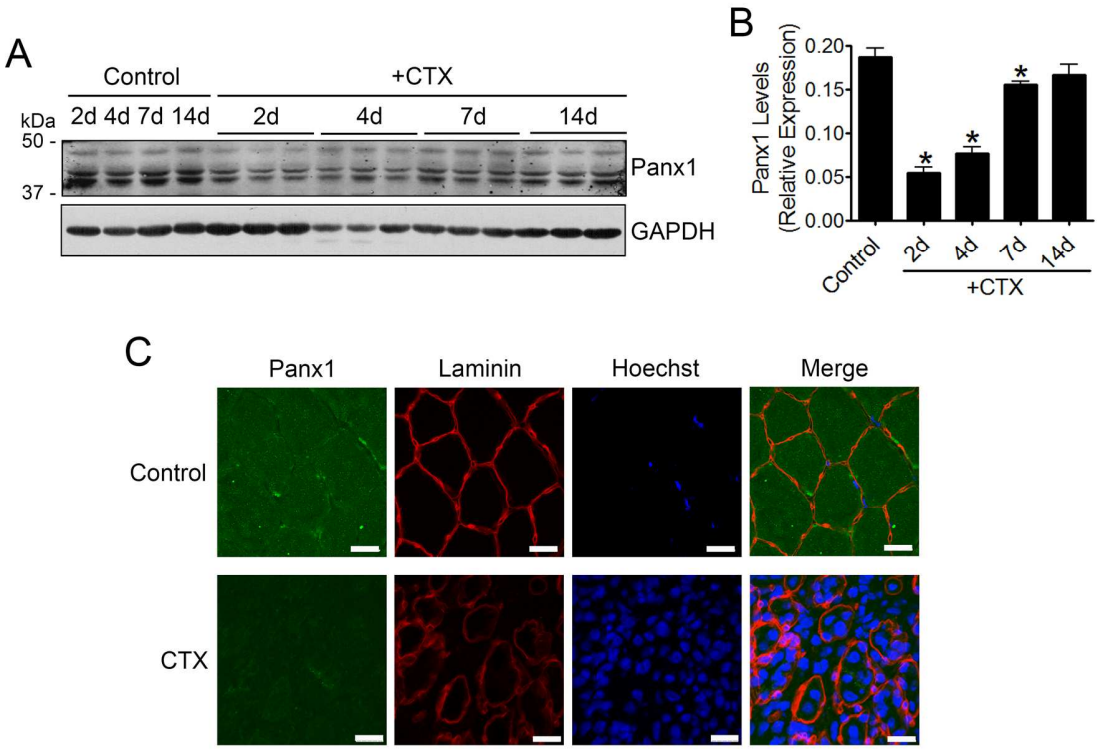

Figure 5. Panx1 levels are modulated during skeletal muscle degeneration/regeneration. (A) Western blots showing Panx1 protein levels in regenerating TA muscle following cardiotoxin (CTX) injection. TA muscles were harvested 2, 4, 7 and 14 d post-injection. Saline-injected muscles (Control) were used as controls. GAPDH was used as a loading control. **(B)** Relative quantification of Panx1 levels (n=3). Panx1 levels decreased at day 2 post-injury and gradually returned to control levels 14 days post-injury when muscle fibers are fully regenerated. Data are mean ± SD, *p≤0.05 compared to Control. **(C)** Cross-sections of TA muscles at 4 d post-injection were labeled for Panx1 (green) and laminin (red). A decrease of Panx1 staining was observed in the regenerating muscle. Blue = nuclei, bars = 10µm.

Similar to muscle development, we interestingly observed a dramatic shift in the Panx3 species expressed during the skeletal muscle degeneration-regeneration process (**Fig. 6A**). Specifically, the lower MM forms of Panx3 were significantly decreased at day 2 post-injury and subsequently gradually increasing to approach that of the saline controls by day 14. By contrast, the ~70 kDa immunoreactive species of Panx3 drastically increased at day 2 post-injury, gradually diminishing and returning to control levels 14 days post-injury (**Fig. 6A-C**). While the Panx3 localization pattern was not changed at day 4 post-injury, there was a general decrease in Panx3 staining throughout the CTX-injected muscles compared to that of the saline controls (**Fig. 6D**). Taken together, these results show a differential modulation of Panx1 and Panx3 levels during skeletal muscle regeneration *in vivo,* further demonstrating that Panx1 and Panx3 are regulated during skeletal myogenesis.

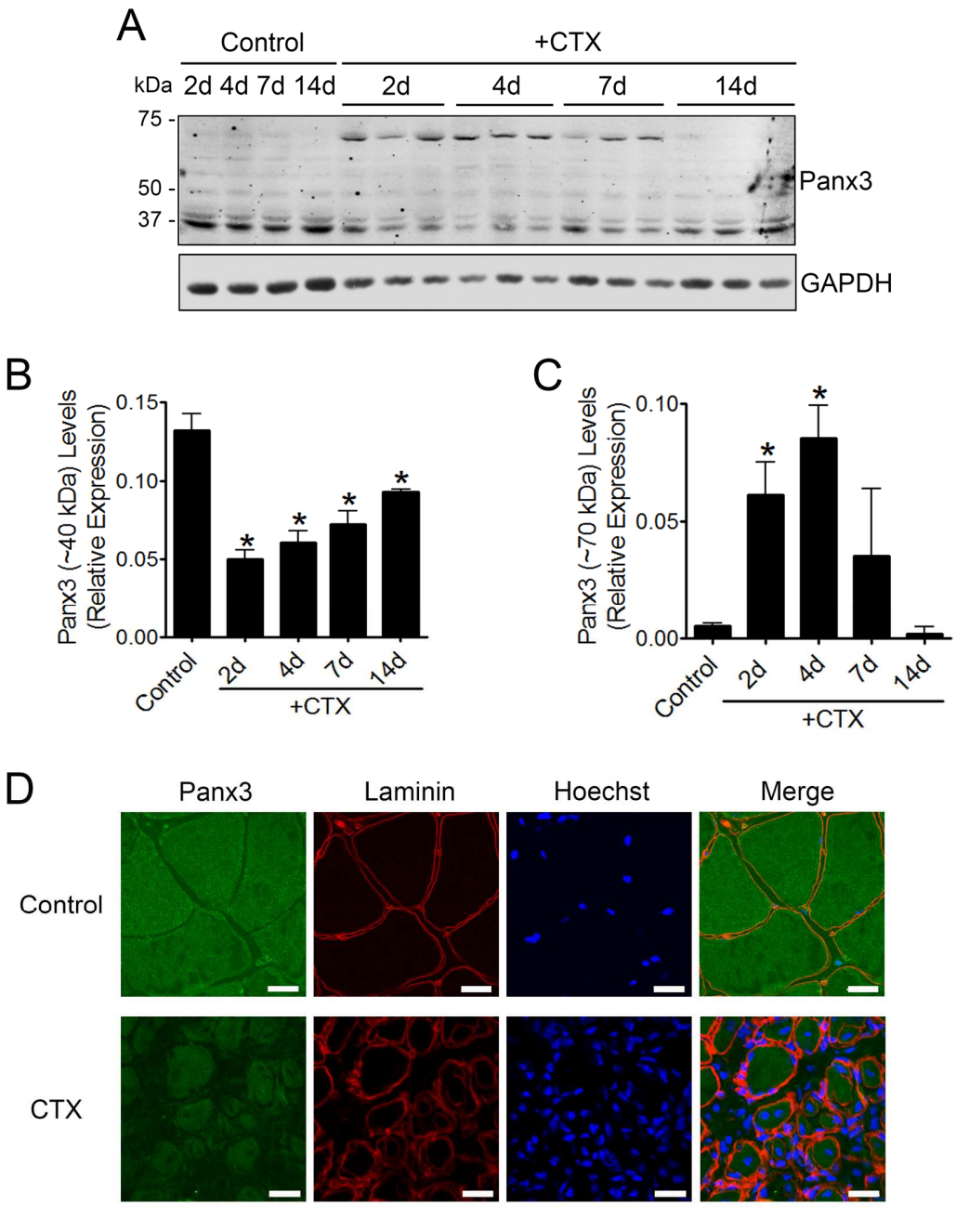

Figure 6. Panx3 levels are modulated during skeletal muscle degeneration/regeneration. (A) Western blots showing Panx3 protein levels in regenerating TA muscle following cardiotoxin (CTX) injection. TA muscles were harvested 2, 4, 7 and 14 d post-injection. Saline-injected muscles (Control) were used as controls. GAPDH was used as a loading control. Relative quantification of the low molecular weight (kDa) species of Panx3 **(B)** as well as of its ~70 kDa immunoreactive species **(C)** (n=3). While the lower MM forms of Panx3 were significantly decreased at day 2 post-injury, gradually increasing close to that of saline controls by day 14, its ~70 kDa immunoreactive species drastically increased at day 2 post-injury, gradually

diminishing and returning to control levels 14 days post-injury. Data are mean ± SD, *p≤0.05 compared to Control. **(D)** Cross-sections of TA muscles at 4 d post-injection were labeled for the lower MM species of Panx3 (green) and laminin (red). A decrease of Panx3 staining was observed in the regenerating muscle. Blue = nuclei, bars = 10µm.

3.5 Panx1 and Panx3 levels are dysregulated in skeletal muscle dystrophy

Since our data indicate that Panx1 and Panx3 levels are regulated during mouse muscle development and regeneration, we next wanted to examine Panx1 and Panx3 levels in a situation where myogenesis is dysregulated such as in Duchenne muscular dystrophy (DMD). We thus compared Panx1 and Panx3 levels in muscles (TA, EDL, and SOL) from *mdx* mice and control animals. As shown in Figure 7, there was a small decrease in Panx1 protein expression in EDL, but not in TA or SOL, from 4-week-old *mdx* mice compared to that of the respective muscles of the parental line (**Fig. 7A-B**). As for Panx3, there was also a significant diminution of its low MM species (~35-40 kDa) levels in dystrophic TA and EDL muscles, together with a drastic increase of its ~70 kDa immunoreactive species in EDL and SOL muscles (**Fig. 7C-E**).

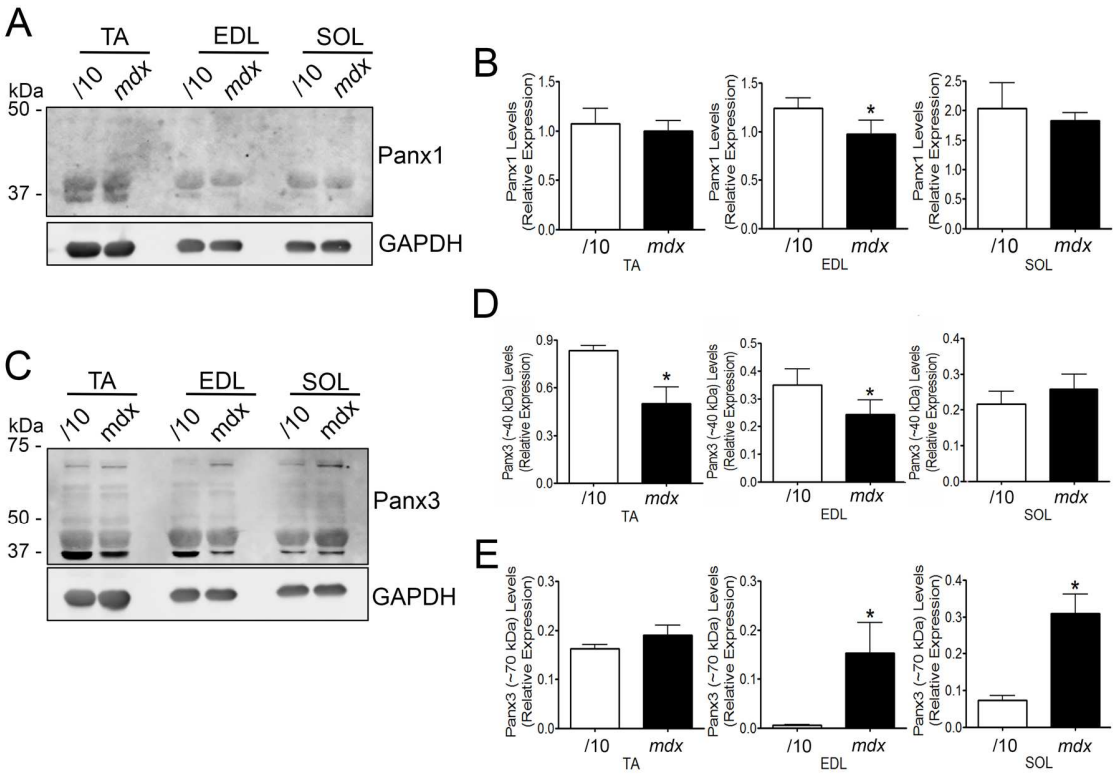

Figure 7. Panx1 and Panx3 levels are regulated in dystrophin-deficient mice. Panx1 and Panx3 protein levels were analyzed by Western blots in different skeletal muscle tissues (TA, EDL, SOL) from dystrophin-deficient mice (*mdx*) as a model for Duchenne muscular dystrophy compared to the parent line, C57BL/10 (/10) at 4 weeks old. Panx1 levels were slightly decreased in dystrophic EDL compared to control mice, while no differences were observed in TA and SOL skeletal muscles **(A-B)**. GAPDH was used as a loading control for relative quantification. Data are mean ± SD, *p≤0.05 (n=4). On the other hand, the levels of the low molecular weight species (~35-40 kDa) of Panx3 were significantly decreased in TA and EDL muscles of *mdx* mice **(C-D)**, while the levels of its ~70kDa immunoreactive species were increased in their EDL and SOL **(C, E)**. GAPDH was used as a loading control for relative quantification. Data are mean ± SD, *p≤0.05 (n=4).

While the *mdx* mouse is a popular model for DMD, its clinical symptoms are minimal in part due to compensation in muscle fibers by functional and structural homologs of dystrophin such as utrophin and its ability to regenerate fibers over a shorter life span [136]. We have thus examined Panx1 and Panx3 levels in TA, EDL, and SOL skeletal muscles of 8-week-old *utrophin/dystrophin dKO* mice as compared to that of control mice. In these studies, we have also included the diaphragm (DPH) as it is the most impaired muscle in DMD, and its wasting is responsible for clinical respiratory failure in DMD patients [178,179]. While there was a trend towards diminution in TA muscles, Panx1 levels were found to be significantly decreased in EDL, SOL, and DPH of *dKO* mice (**Fig. 8A-B**). Importantly, Panx3 levels were significantly altered in all muscles examined with its low MM species being decreased and its ~70 kDa immunoreactive species being strikingly elevated (**Fig. 8C-E**).

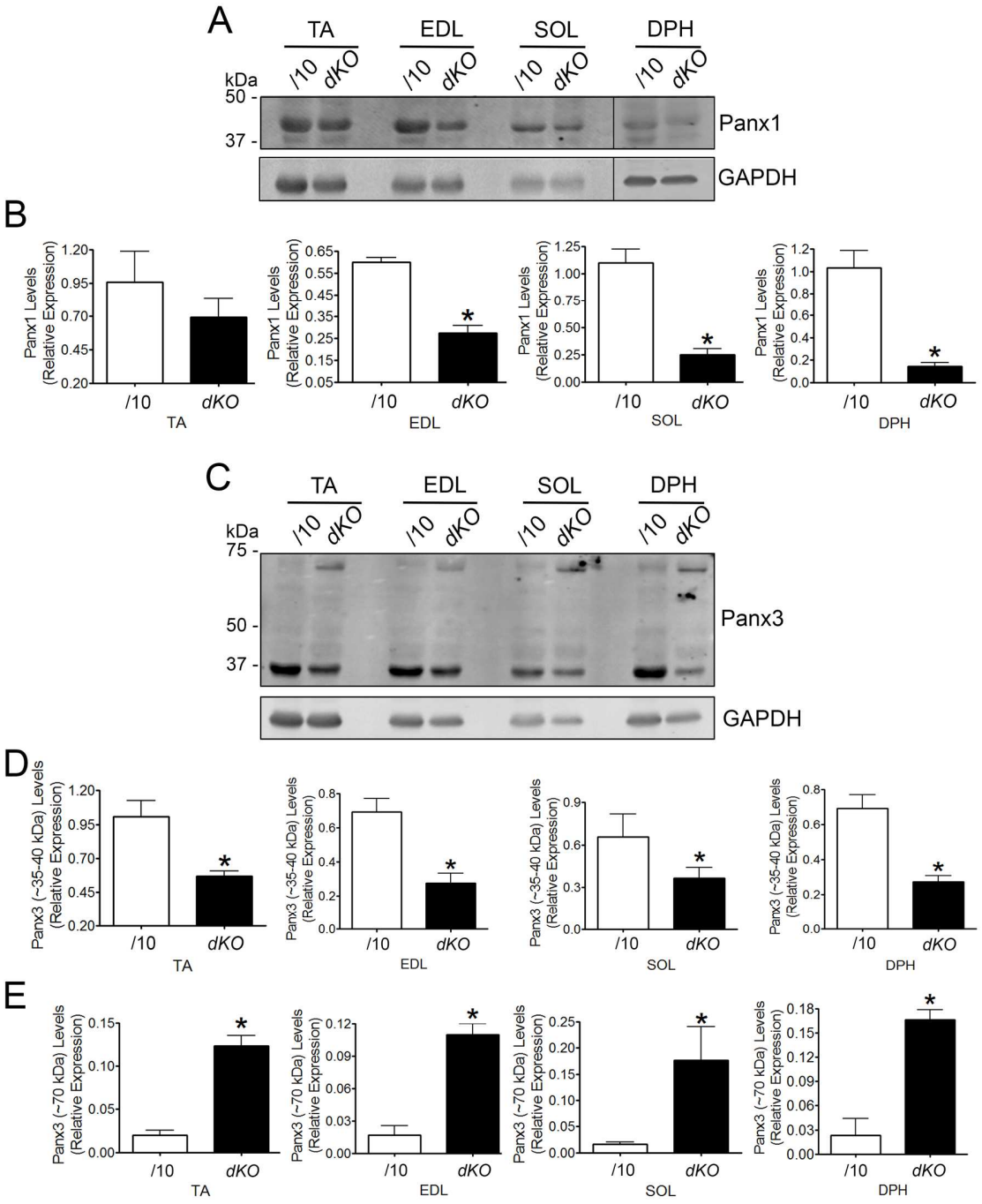

Figure 8. Panx1 and Panx3 levels are down-regulated in utrophin/dystrophin-deficient mice. Panx1 and Panx3 protein levels were analyzed by Western blots in TA, EDL, SOL, and diaphragm (DPH) from utrophin/dystrophin-deficient mice (*dKO*) compared to the parent line, C57BL/10 (/10) at 8 weeks old. Panx1 levels were significantly decreased in EDL, SOL, and DPH from dystrophic mice compared to controls **(A-B)**. GAPDH was used as a loading control for relative quantification. Data are mean ± SD, *p≤0.05 (n=3). The levels of the low molecular weight species (~35-40

kDa) of Panx3 were significantly decreased in all dystrophic muscles assessed **(C-D)**, while the levels of its ~70kDa immunoreactive species were drastically increased **(C, E)**. GAPDH was used as a loading control for relative quantification. Data are mean ± SD, *p≤0.05 (n=3).

To assess whether Panx1 localization is altered in SCs in *dKO* mice compared to their control, cross-sections from all muscles examined were immunolabeled for Panx1 (green) and Cav-1 (red), a marker of SCs [180]. Panx1 localization was consistent between *dKO* and control sections where Panx1 was localized throughout the myofibers with areas of increased punctate staining near the membrane not necessarily associated to SCs (**Fig. 9**). There were no differences in the level of Panx1 staining in TA, which histologically is most similar to the control in terms of maintenance of organized myofiber architecture. In EDL, SOL and DPH from *dKO* mice; however, there were mostly areas of decreased Panx1 labelling with the occasional area of increased staining (**Fig. 9**). Here, DPH was the most affected muscle observed in terms of loss of myofiber structure and had the most decreased level of Panx1 staining. To further investigate whether these differences in Panx1 immunolabelling were associated to histologically healthy (characterized by organized myofibers structure with peripherally-located nuclei), regenerating (characterized by organized myofibers structure with centrally-located nuclei) or inflammatory/necrotic (characterized by loss of myofiber structure and infiltration of non-muscle mononuclear cells) muscle in *dKO* mice [61,136], we performed a hematoxylin and eosin stain (H&E) of EDL cross-sections. The histology of *dKO* muscles comprised of mostly healthy (h) and regenerating (r) areas, which had decreased Panx1 staining (green), while inflammatory/necrotic (i) areas made up a smaller composition of the *dKO* muscles but had increased Panx1 staining (**Fig. 10)**.

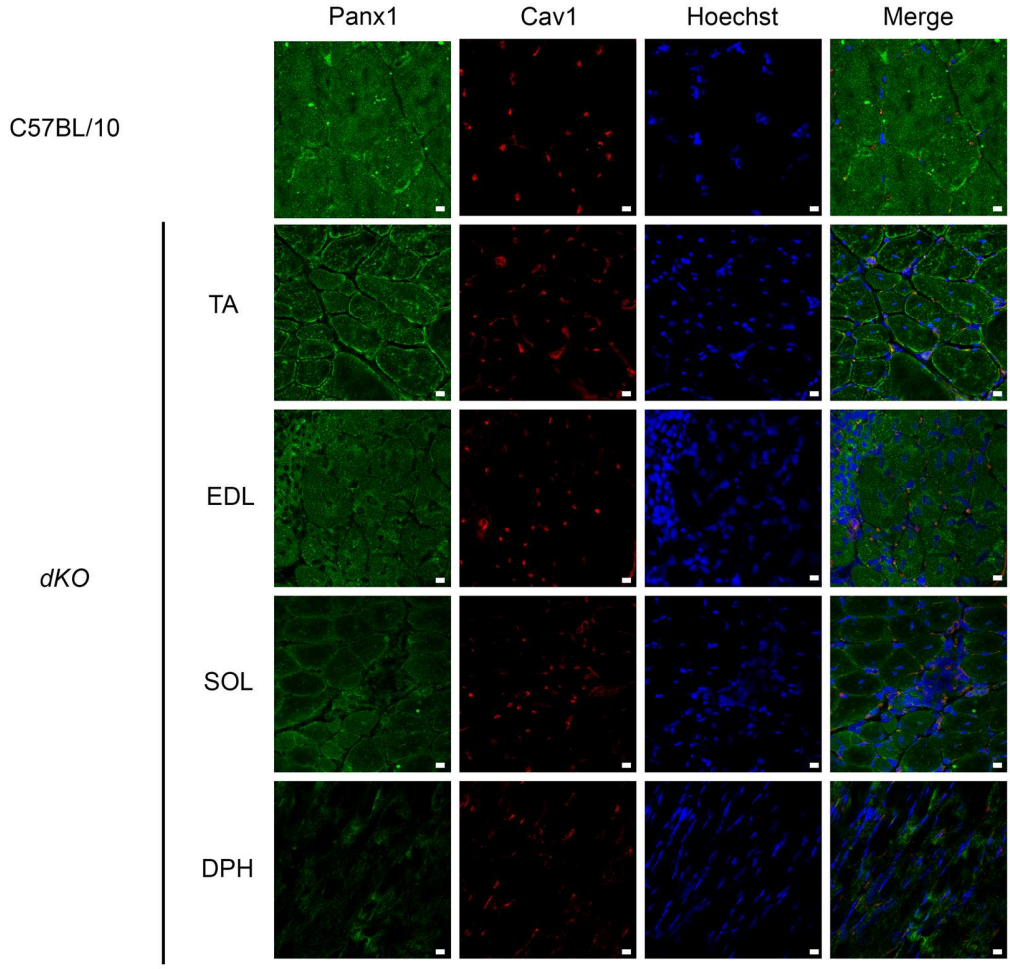

Figure 9. Panx1 localization is not altered in utrophin/dystrophin-deficient mice. Cross-sections of TA, EDL, SOL, and DPH muscles from *dKO* mice and the parent line, C57BL/10, at 8 weeks old were labeled for Panx1 (green) and Cav1 (red). While Panx1 localization was consistent in all muscles studied from the *dKO* mice and the parent line, there was a general decrease in Panx1 staining in EDL, SOL, and DPH; however, there were a few small areas in all muscles studies with increased Panx1 staining. Blue = nuclei, bars = 10µm (n=3).

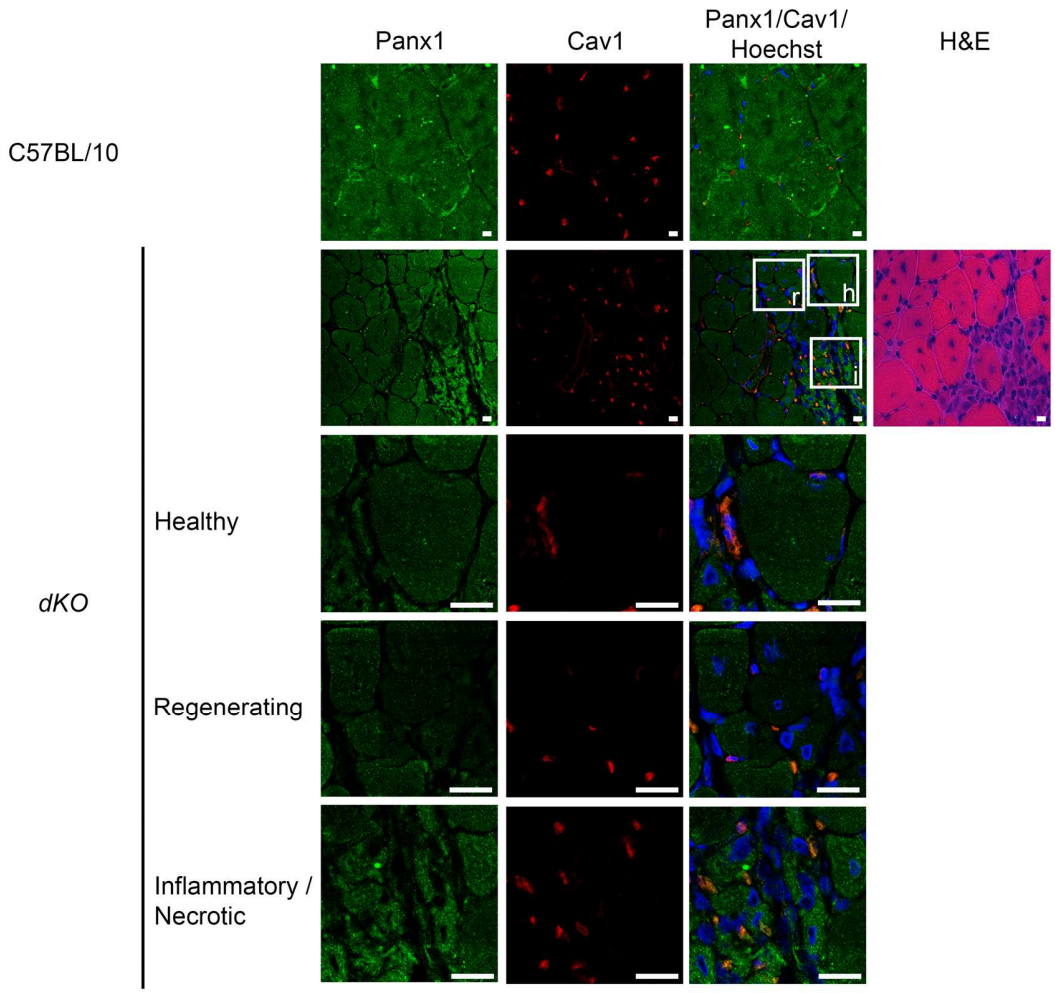

Figure 10. Panx1 levels are down-regulated in histologically healthy and regenerating areas of muscle from utrophin/dystrophin-deficient mice, and up-regulated in histologically inflammatory/necrotic areas. Cross-sections of EDL muscles from *dKO* mice and the parent line at 8 weeks old were labeled for Panx1 (green) and Cav1 (red), and stained with hematoxylin and eosin (H&E). Histologically healthy areas (white inset labelled "h") (organized myofibers structure and peripherally-located nuclei) and histologically regenerating areas (white inset labelled "r") (organized myofibers structure with centrally-located nuclei) showed decreased Panx1 staining, while inflammatory/necrotic areas (white inset labelled "i") (disorganized myofibers structure and infiltration of mononuclear cells) had increased Panx1 staining compared to the parent line. Blue = nuclei, bars = 10µm (n=3).

To assess whether Panx3 localization is altered in SCs in *dKO* mice compared to their control, cross-sections from all muscles examined were immunolabeled for Panx3 (green) and Cav-1 (red). While Panx3 localization pattern was not changed in *dKO* muscles compared to controls, there was a reduction in Panx3 staining level in TA, EDL, SOL and DPH (**Fig. 11**) likely representing the low MM species of Panx3 as the antibody is not expected to detect the ~70 kDa immunoreactive species of Panx3 in immunofluorescent staining [5]. This reduction in Panx3 staining intensity seems specific to areas of histologically healthy (h) and regenerating (r) muscle, while the few small areas of histologically inflammatory/necrotic (i) muscle demonstrated increased Panx3 labelling (**Fig. 12**). Altogether, our data revealed that Panx1 and Panx3 levels are dysregulated in muscular dystrophy.

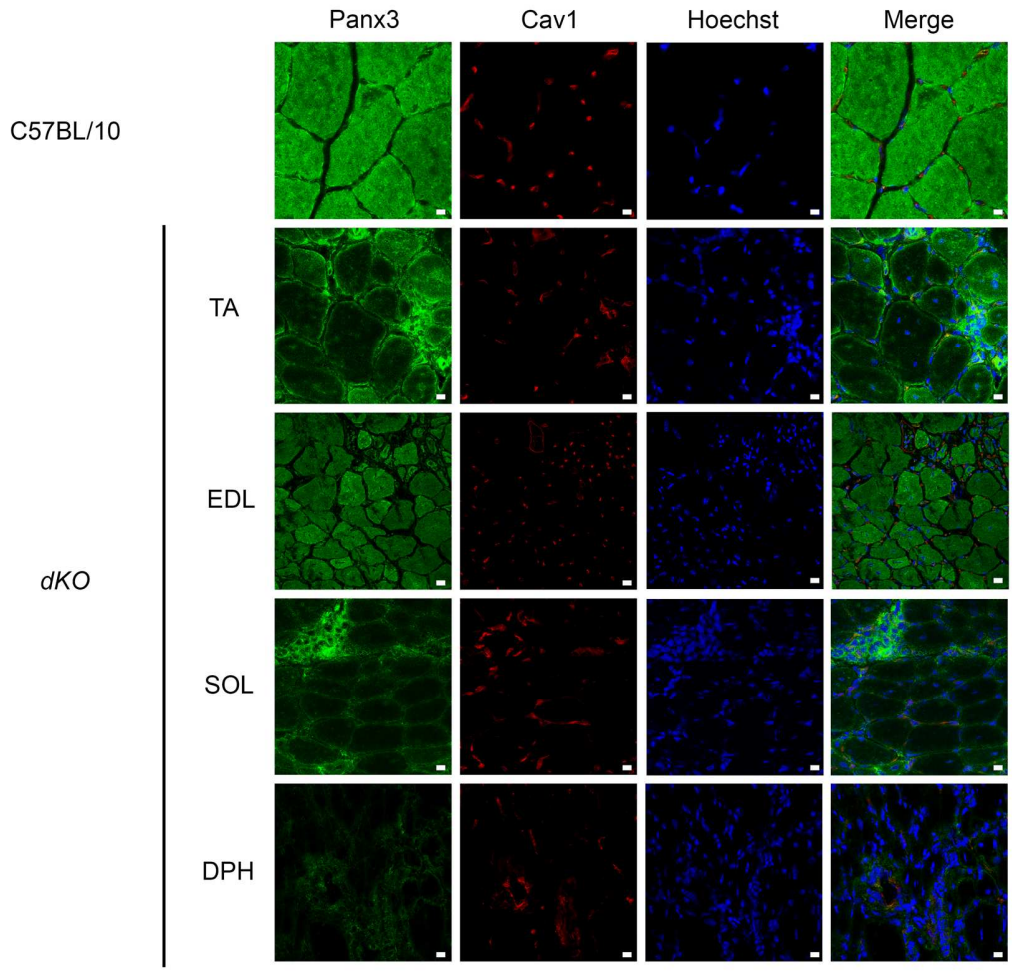

Figure 11. Panx3 localization is not altered in utrophin/dystrophin-deficient mice. Cross-sections of TA, EDL, SOL, and DPH muscles from *dKO* mice and the parent line, C57BL/10, at 8 weeks old were labeled for Panx3 (green) and Cav1 (red). While Panx3 localization was consistent in all muscles studied from the *dKO* mice and the parent line there was general decrease in Panx3 staining in TA, EDL, SOL, and DPH; however, there were a few small areas in all muscles studied with increased Panx3 staining. Blue = nuclei, bars = 10µm (n=3).

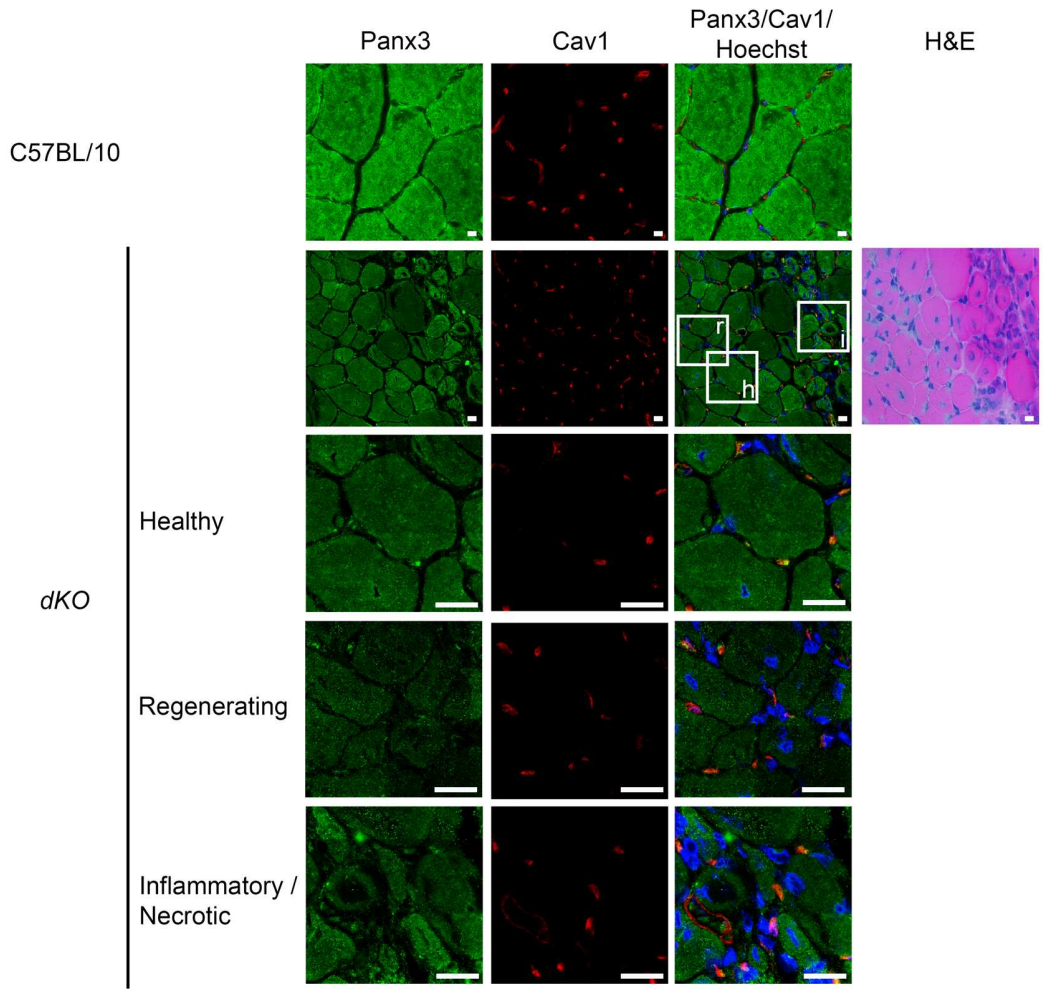

Figure 12. Panx3 levels are down-regulated in histologically healthy and regenerating areas of muscles from utrophin/dystrophin-deficient mice, and up-regulated in histologically inflammatory/necrotic areas. Cross-sections of EDL muscles from *dKO* mice and the parent line at 8 weeks old were labeled for Panx3 (green) and Cav1 (red), and stained with hematoxylin and eosin (H&E). Histologically healthy areas (white inset labelled "h") (organized myofibers structure and peripherally-located nuclei) and histologically regenerating areas (white inset labelled "r") (organized myofibers structure with centrally-located nuclei) showed decreased Panx3 staining, while inflammatory/necrotic areas (white inset labelled "i") (disorganized myofibers structure and infiltration of mononuclear cells) had increased Panx3 staining compared to the parent line. Blue = nuclei, bars = 10µm (n=3).

3.6 PANX1 inhibition supresses SC differentiation

Given our previous finding that PANX1 over-expression induces myoblast differentiation, while blocking its channel activity using probenecid or carbenoxolone

inhibited this process [14], we wanted to determine whether PANX1 channels regulate the differentiation of SCs as well as possibly promoting myogenesis during muscle development and regeneration. PANX1 is expressed in human SCs (**Fig. 4A**) and is localized as punctate structures throughout the cell with increased labeling at the cell surface, mainly at cell-to-cell interactions (**Fig. 13A**). Prior to induction of differentiation, upwards of 95% of human SCs express MyoD with upwards of 60% of cells being double positive for Pax7 and MyoD ($Pax7^{+}MyoD^{+}$) between passages 0 and 6 (**Fig. 13B**); therefore, these human SCs are considered activated [103] at the start of the assay. When human SCs were differentiated in serum-deprived differentiation media for 6 days to form myotubes, PANX1 (green) was expressed in all the cells throughout the differentiation assay from D0 to D6, but quantification of the MYOG-positive cells (red) suggests increased levels of PANX1 labelling at D6 compared to MYOG-negative cells at D0 and D6 (**Fig. 14A-B**). Similarly, quantification of MHC-positive cells (red) suggests increased PANX1 labelling at D6 compared to MYOG-negative cells at D0 and D6 (**Fig. 14C-D**). As expected during SC differentiation, an increase in fused multinucleated cells was observed at day 6 (D6) compared to day 0 (D0), where undifferentiated SCs are largely $Pax7^{+}MyoD^{+}$ and fused multinucleated cells express the early differentiation marker MyoD but not the SC marker Pax7 upon immunolabeling (**Fig. 15A**). 1mM of probenecid or 100µM of carbenoxolone compared to PBS controls were used to block PANX1 channels and study their effects on early differentiation of human SCs. The percentage of $Pax7^{+}MyoD^{+}$ cells was 78% at D0 and decreased to 33% after 6 days of differentiation, while treatment with probenecid or carbenoxolone did not significantly affect the $Pax7^{+}MyoD^{+}$ population (**Fig. 15B-C**) nor the Pax7-MyoD+

population at D6 (**Fig. 15B,D**) suggesting that Panx1 is not involved in maintaining the activated SC population and induction of early differentiation, though it is still unknown whether Panx1 may still play a role in maintaining the $Pax7^{+}$ quiescent SC population.

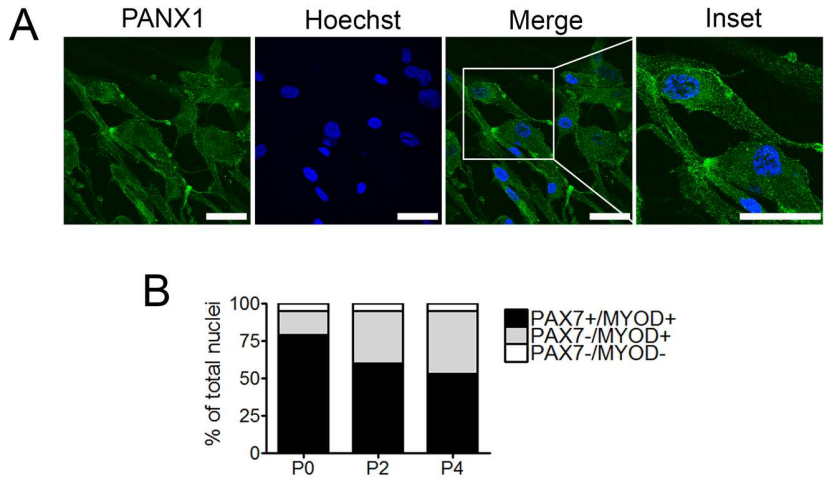

Figure 13. Characterization of human primary skeletal muscle SCs. Human primary skeletal muscle SCs labelled with PANX1 (green) demonstrated that PANX1 is localized as punctate structures throughout the cell with increased staining at cell-to-cell interactions **(A)**. SCs labelled with Pax and MyoD at passages 0, 2 and 4 (P0, P2 and P4) showed that upwards of 95% of SCs express MYOD with upwards of 60% of cells being double positive for PAX7 and MYOD between passages 0 and 6; therefore, these human SCs are considered activated [103] at the start of the assay **(B)**.

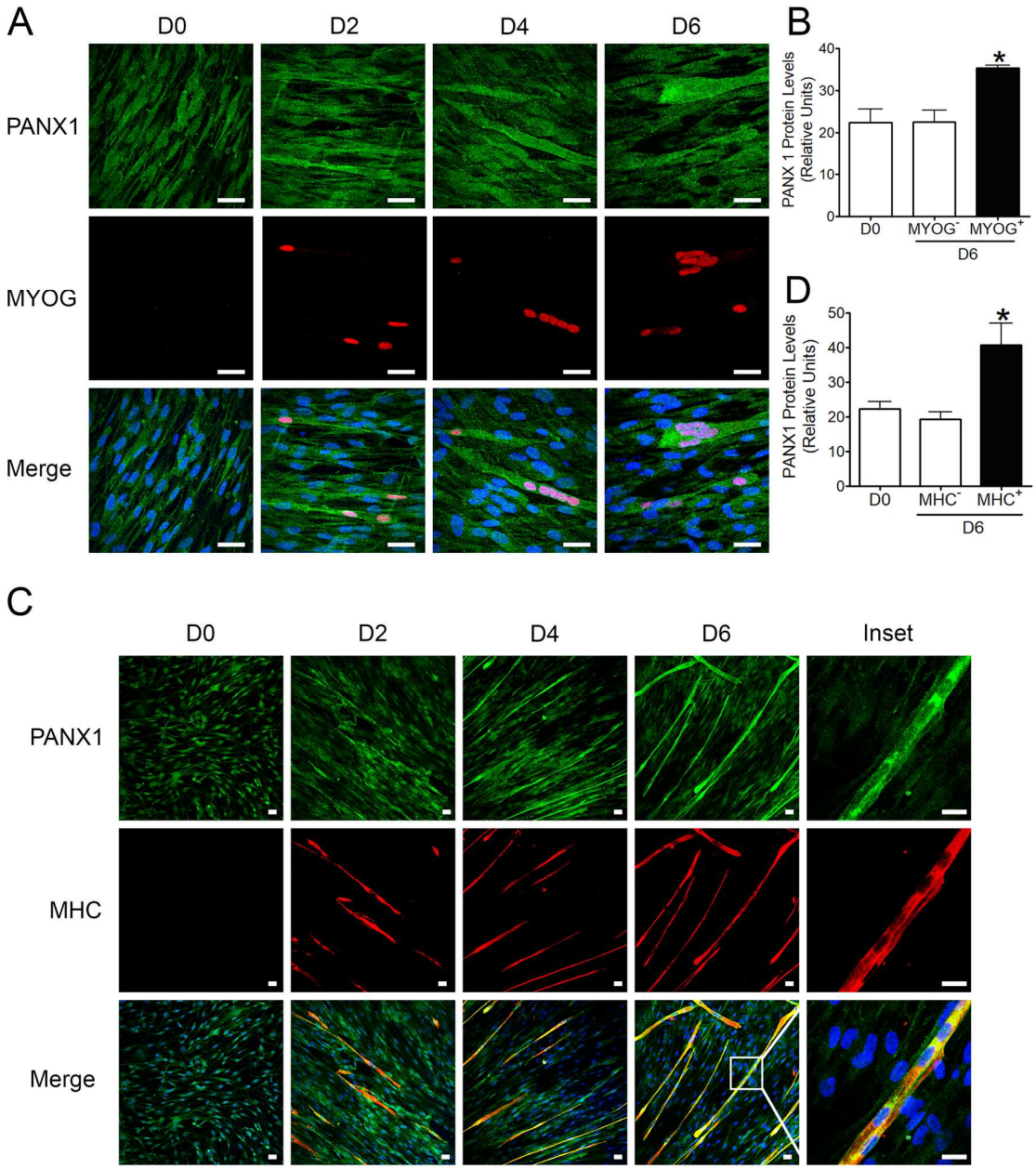

Figure 14. PANX1 levels increase during SC differentiation. Human primary skeletal muscle SCs were differentiated over a course of 6 days in serum-deficient differentiation media and labeled with PANX1 (green) and myogenin (MyoG) (red) **(A)** at days 0, 2, 4, and 6 (D0, 2, 4, 6). PANX1 staining was increased in MYOG-positive cells ($MYOG^+$) at D6 compared to MYOG-negative cells ($MYOG^-$) at D0 and D6 **(B)**. Similarly, PANX1 labelling was increased in myosin heavy chain (MHC)-positive cells (MHC^+) (red) **(C)** at D6 compared to MHC-negative cells (MHC^-) at D0 and D6 **(D)**. Data are mean ± SD, *p≤0.05 (n=3) Blue = nuclei, bars = 10µm. Data are mean ± SD, *p≤0.05 (n=3).

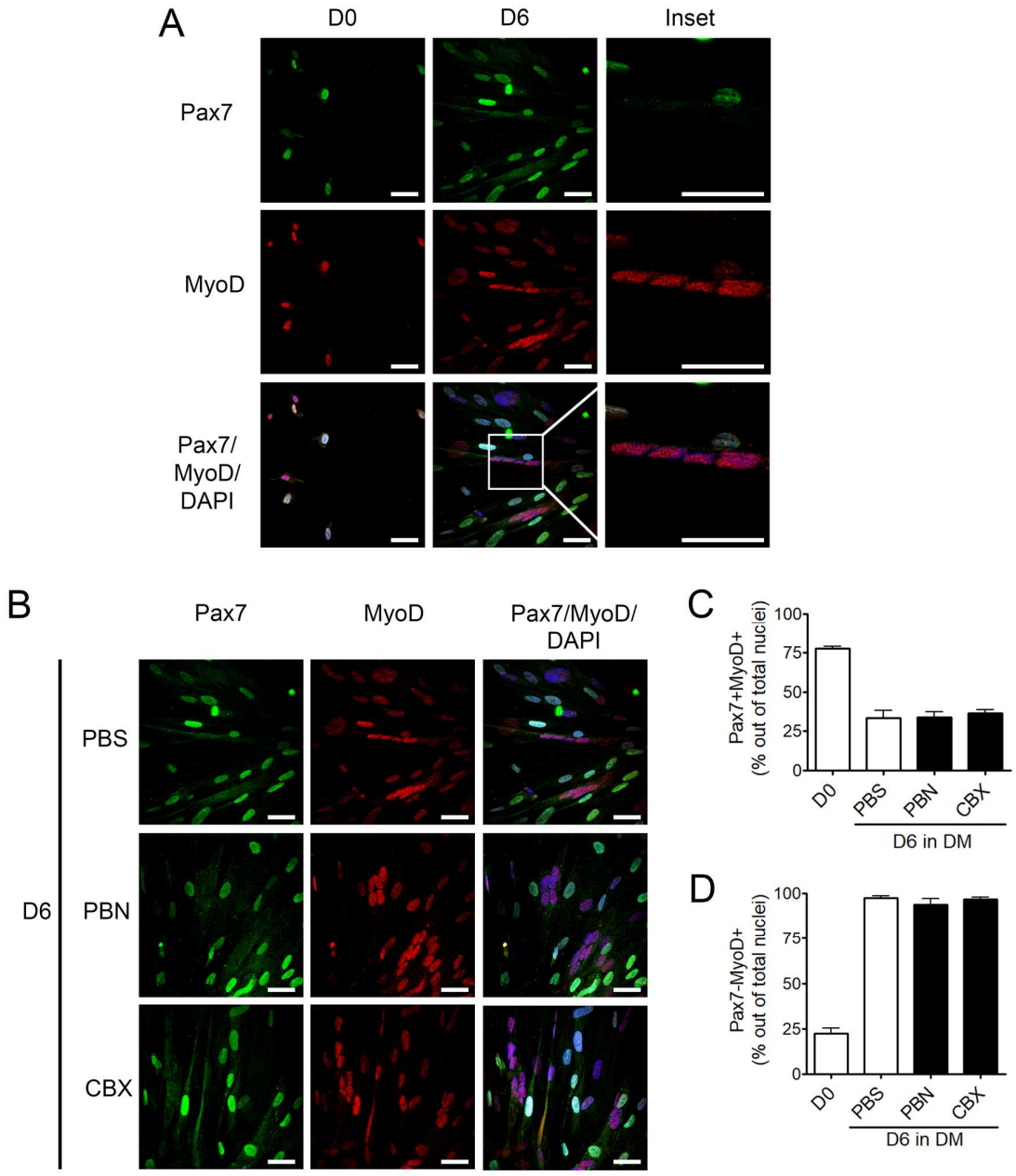

Figure 15. PANX1 inhibition does not affect the percentage of Pax7^{+}MyoD^{+} SCs and early differentiating Pax^{-}MyoD^{+} SCs. Human primary skeletal muscle SCs were differentiated over a course of 6 days in serum-deficient media without PANX1 channel inhibitors **(A)** or with PANX1 channel blockers, probenecid (PBN) or carbenoxolone (CBX), and vehicle control, PBS **(B)**. Cells were labelled with Pax7 (green) and MyoD (red) at days 0 and 6 (D0 and D6). Blue = nuclei, bars = 10µm. As expected, cells were largely Pax7^{+}MyoD^{+} at D0, whereas more cells at D6 were fused and multinucleated becoming Pax7^{-}MyoD^{+}. There were no significant differences in the Pax7^{+}MyoD^{+} **(C)** and Pax7^{-}MyoD^{+} **(D)** populations compared to controls when human SCs were treated

with PBN or CBX during differentiation suggesting that PANX1 is not involved in early differentiation and maintenance of the activated SC population. Data are mean ± SD, *p≤0.05 (n=3).

To study the effect of PANX1 channel blockers probenecid and carbenoxolone on late differentiation of human SCs, SCs were labeled for the late differentiation marker MyoG (red) as well as the terminal differentiation marker MHC (red). At D0, cells did not express MyoG, but 7% of cells were positive for MyoG at D6, which decreased by 32% and 75% upon probenecid and carbenoxolone treatment, respectively (**Fig. 16A-B**). Similarly, cells did not express MHC at D0, but 9% of cells were MHC-positive at D6 (**Fig. 17A-B**). This differentiation index was significantly decreased by 15% and 52% upon probenecid and carbenoxolone treatment compared to controls, respectively (**Fig. 17A-B**), while the fusion index decreased by 35% and 54% (**Fig. 17A,C**). Furthermore, probenecid or carbenoxolone treatments significantly shifted the proportion of MHC-positive cells from high level multinucleation (10-25+ nuclei) (significant decrease) towards a population with low level multinucleation (2-4 nuclei) (significant increase) as compared to controls (**Fig. 17D-F**). Specifically, the proportion of MHC-positive cells with low level of nucleation increased by 1.6X and 2.1X upon probenecid or carbenoxolone treatment compared to controls (**Fig. 17D**), respectively, while the proportion of MHC-positive cells with high level of nucleation decreased by 45% and 72% (**Fig. 17F**), respectively. Furthermore, carbenoxolone but not probenecid significantly decreased the proportion of MHC-positive cells with moderate multinucleation (5-9 nuclei) by 45% (**Fig. 17F**). Taken together, blocking PANX1 channels may inhibit human SC differentiation and fusion.

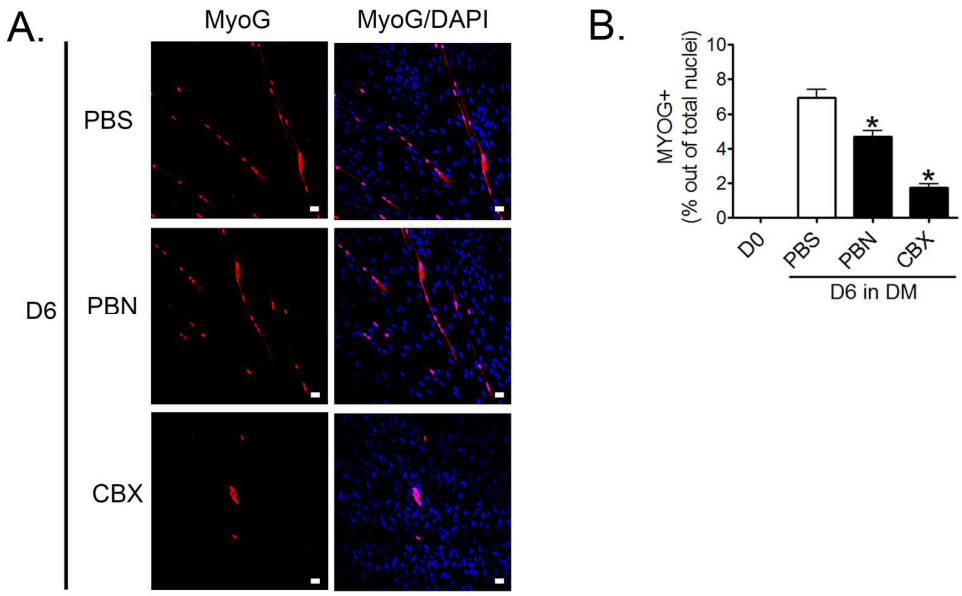

Figure 16. PANX1 inhibition decreases the percentage of differentiating SCs expressing the late differentiation marker myogenin. Human primary skeletal muscle SCs were differentiated over a course of 6 days in serum-deficient media with PANX1 channel blockers, probenecid (PBN) or carbenoxolone (CBX), and vehicle control, PBS. Cells were labeled with myogenin (MyoG) (red) at day 6 (D6). Blue = nuclei, bars = 10µm **(A)**. The percentage of MyoG-positive cells decreased when human SCs were treated with probenecid (PBN) or carbenoxolone (CBX). Data are mean ± SD, *p≤0.05 (n=3).

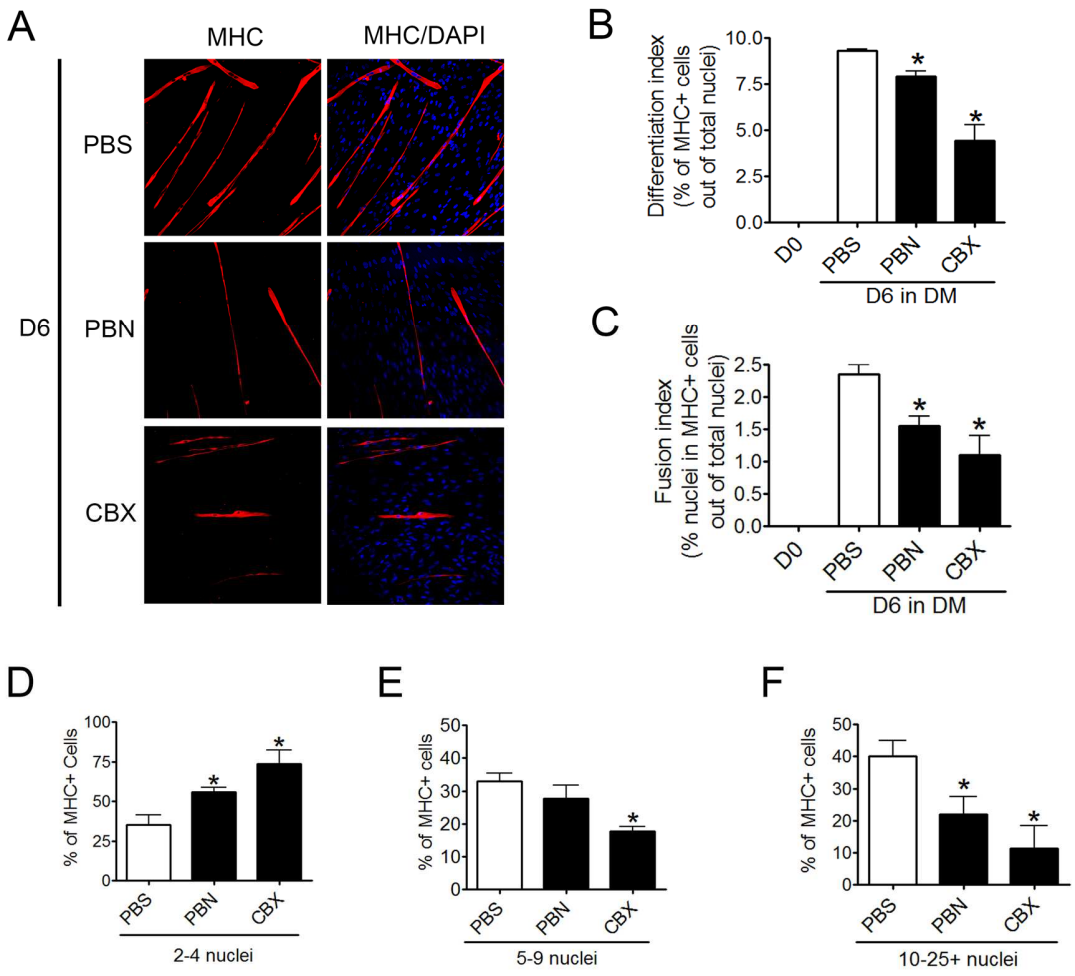

Figure 17. PANX1 inhibition decreases indices of SC late differentiation. Human primary skeletal muscle SCs were differentiated over a course of 6 days in serum-deficient media with PANX1 channel blockers, probenecid (PBN) or carbenoxolone (CBX), and vehicle control, PBS. Cells were labelled with myosin heavy chain (MHC) (red) at day 6 (D6). Blue = nuclei, bars = 10µm **(A)**. The differentiation index **(B)** and the fusion indexes **(C)** were significantly decreased upon probenecid and carbenoxolone treatment during human SC differentiation. Probenecid and carbenoxolone also significantly increased the percentage of MHC+ cells with 2-4 nuclei, while decreasing the percentage of MHC-positive cells with 10-25+ nuclei; carbenoxolone significantly decreased the percentage of MHC-positive cells with 5-9 nuclei **(D-F)**. Data are mean ± SD, *$p \leq 0.05$ (n=3).

3.7 PANX1 inhibition reduces SC proliferation

While our previous data showed that PANX1 does not regulate myoblast proliferation, as probenecid, carbenoxolone, and PANX1 over-expression did not have an effect on this process [14], I wanted to determine whether PANX1 channels instead regulate SC proliferation. When human SCs were treated with probenecid in proliferation assays, the level of BrdU incorporation decreased by 45% and 74% based on immunofluorescent staining (**Fig. 18A-B**) and ELISA assays (**Fig. 18C**), respectively. BrdU incorporation was similarly decreased by 94% after carbenoxolone treatment in ELISA assays (**Fig. 18D**). Altogether, our data suggests that inhibition of PANX1 channels suppresses human SC proliferation.

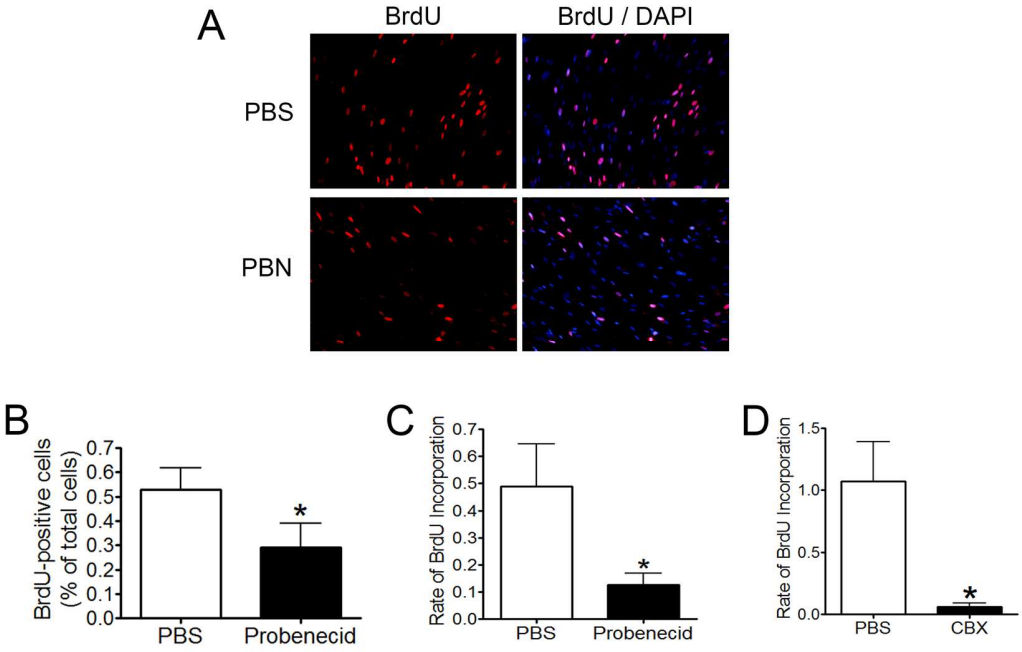

Figure 18. PANX1 inhibition decreases SC proliferation. Human primary SCs were treated with 1mM probenecid (PBN) or PBS control for 24 hours and pulsed with 5-bromo-2-deoxyuridine (BrdU) for 2 hours, followed by BrdU staining (red) **(A)**. The percentage of BrdU-positive cells was significantly decreased upon probenecid treatment

compared to controls **(B)**, and analysis by BrdU-ELISA also revealed that the level of BrdU incorporation was decreased upon probenecid treatment **(C)** and upon carbenoxolone treatment **(D)**.

4.0 DISCUSSION

In the present study, we show that expression of Panx1 is low in embryonic mouse skeletal muscle and increases progressively thereafter to become highly expressed in juvenile and adult muscle. In contrast, the low MM species of Panx3 maintained similar levels throughout muscle development. However, the ~70 kDa immunoreactive species of Panx3, which was detected in embryonic muscle, decreased drastically during development resulting in low levels in mature adult muscle. This expression pattern is similar to that previously reported by our laboratory in human fetal versus adult skeletal muscle tissue [14], during SkMC (primary human skeletal muscle cells) and HSMM (human primary skeletal muscle myoblasts) differentiation [14], as well as in our muscle degeneration/regeneration experiments. The levels of both Panx1 and the lower MM form of Panx3 drastically decrease upon skeletal muscle degeneration and gradually increase during regeneration, while the levels of the ~70 kDa immunoreactive species of Panx3 drastically increases during degeneration and gradually decreases during regeneration. Altogether, these findings summarized in **Figure 19** demonstrate that the levels of Panx1 and Panx3 are tightly and distinctly regulated during muscle development and regeneration.

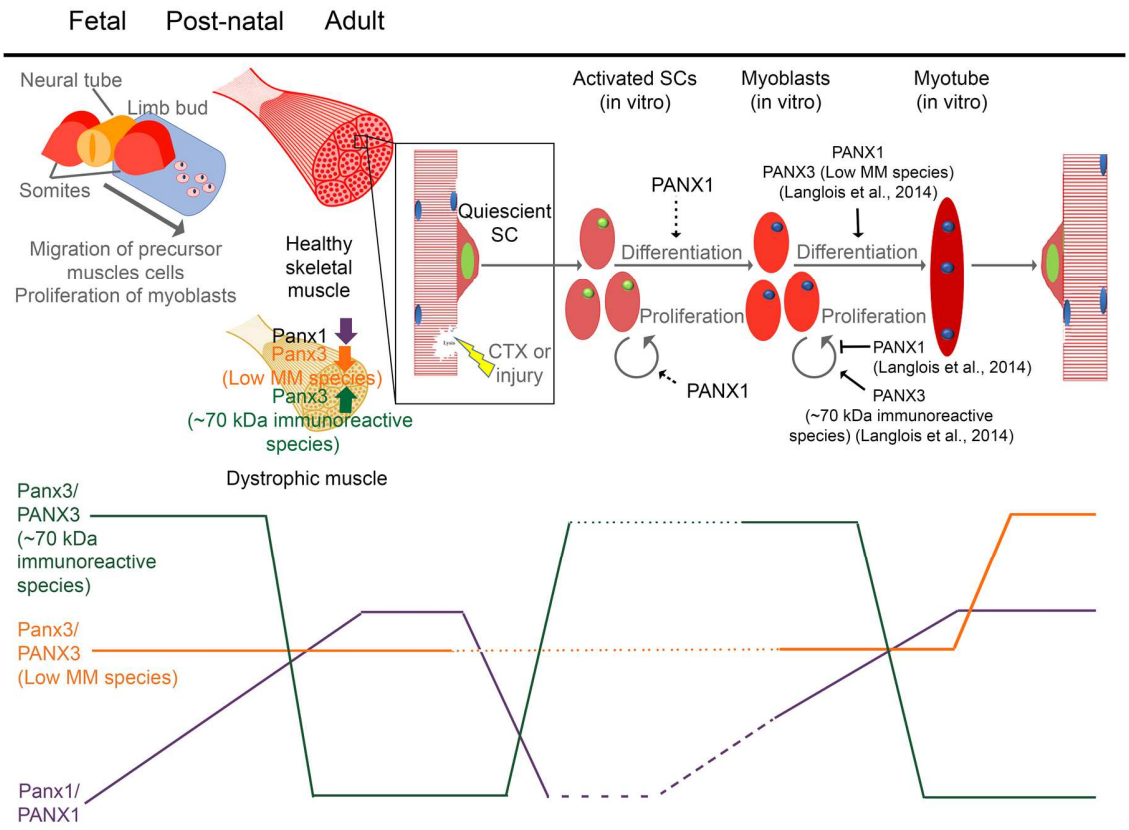

Figure 19. Panx1/PANX1 and Panx3/PANX3 levels are modulated during differentiation and proliferation of both skeletal muscle myoblasts and SCs, regulating the differentiation of myoblasts and the differentiation and proliferation of SCs. In fetal tissue, proliferative myoblasts are the main contributor of pre-muscle growth and our data show that Panx1 expression is low in fetal tissue and gradually increases in post-natal to adult tissue (purple line), which is mainly differentiated and quiescent. In fetal and post-natal tissue, the higher ~70 kDa immunoreactive species of Panx3 is most prominently expressed, but its levels drastically diminish in adulthood (green line), while its lower MM species is stably expressed at low levels throughout development (orange line). During skeletal muscle regeneration, injury or cardiotoxin (CTX) injection to the adult muscle activates quiescent SCs, during which PANX1 levels decrease (purple line), to proliferate and differentiate into myoblasts. Activated SCs *in vitro* demonstrated increasing PANX1 levels during differentiation (dashed purple lines) which may regulate this process. Myoblast proliferation is inhibited by PANX1 and promoted by the ~70 kDa immunoreactive species of PANX3. During myoblast differentiation, PANX1 levels gradually increases (purple lines) while the ~70 kDa immunoreactive species of PANX3 drastically decreases (green lines) with little to no expression of its lower MM form present throughout differentiation [14]. Myoblast differentiation is promoted by PANX1 and the lower MM species of PANX3 *in vitro* [14]. *In vivo*, skeletal muscles treated with CTX to induce degeneration/regeneration first enter a proliferation phase followed by a differentiation phase. These changes were associated with drastically decreased levels of both Panx1 and the lower MM form of Panx3

followed by a gradual increase back to or towards control levels during regeneration. By contrast, the ~70 kDa immunoreactive species of Panx3 drastically increased in expression upon CTX-injection and gradually decreased back to control levels in accordance with the *in vitro* results. Dotted lines predict PANX3 levels during SC proliferation and differentiation. In adult dystrophic muscle where regeneration is impaired, expression of Panx1 (purple arrow) and the lower MM species of Panx3 (orange arrow) are decreased compared to that of healthy muscle whereas the expression of the ~70 kDa immunoreactive species of Panx3 is increased (green arrow). Altogether, our data here and data from *Langlois et al.* suggest that Panx1/PANX1 plays an important role in myoblast and SC differentiation during embryonal and adult myogenesis, the lower MM species of Panx3/PANX3 plays a role in maintaining differentiated myoblasts in a differentiated and non-proliferative state throughout development and especially during regeneration, and the ~70 kDa immunoreactive species of Panx3/PANX3 may play a role in keeping undifferentiated myoblasts in a proliferative state during development and regeneration [14].

Previous work from my laboratory established that over-expression of Panx1 induces myoblast differentiation, while blocking its channel activity using probenecid or carbenoxolone inhibited this process [14]. In addition to myoblasts [14], I demonstrate here that mouse and human SCs also express Panx1/PANX1, PANX1 levels may be modulated during SC differentiation (purple dashed lines in **Fig. 19**), and inhibiting PANX1 channels with probenecid or carbenoxolone inhibits the differentiation and proliferation of human SCs. It has been recently shown that Panx1 channels mediate the acquisition of myogenic commitment promoted by ATP release and P_2X receptor activation in murine C_2C_{12} reserve cells, which share many characteristics with SCs [153]. My quantification of PANX1 immunolabelling during differentiation suggest that PANX1 levels are increased in human SCs expressing late and terminal differentiation makers. While Western blot analysis is necessary to further confirm whether PANX1 levels increase during SC differentiation, it is likely that PANX1 levels are gradually increased in SCs and myoblasts to promote myogenesis; thus, accounting for the increasing PANX1 levels during development and regeneration (summarized in **Fig. 19**).

Furthermore, our previous work established that Panx1 does not regulate myoblast proliferation as no effects were observed upon Panx1 over-expression nor inhibition of channel activity with probenecid or carbenoxolone [14]; however, I have shown here that PANX1 channel blockers probenecid or carbenoxolone inhibit SC proliferation, suggesting a tight regulation of PANX1 in order to balance the proliferation and differentiation processes distinguished in myoblasts and SCs. While further confirmation of this is warranted using selective PANX1 channel blockers such as ^{10}Panx mimetic peptide [50], using shRNA to knockdown PANX1, or using a PANX1 over-expression system, one can speculate that PANX1 may affect specific proteins and/or genes downstream that are distinct between myoblasts and SCs resulting in the observed differential effect. For example, Notch signalling has also been shown to play various roles in the differentiation and proliferation of myoblasts versus SCs. Early reports demonstrated that Notch inhibited C_2C_{12} myoblast differentiation, without affecting myoblast proliferation markers, Pax3 or Myf-5 [181,182]. In contrast, Notch promotes proliferation in murine primary cultured SCs [183,184]. Interestingly, Notch signalling has also been implicated in the asymmetric division of SCs producing distinct daughter cells as the committed daughter cell highly expresses DII1, an extracellular ligand of the Notch receptor, which presumably activates Notch signalling in the neighbouring cell since the self-renewed daughter cell is enriched with Notch3 [111]. In future directions, studying the involvement of PANX1 in SC asymmetric self-renewal and commitment would help address the conflicting observations reported here.

While we have also shown that over-expression of the low MM species of Panx3 accelerates myoblast differentiation while inhibiting proliferation [14], our findings

presented here suggest that its levels are not regulated during skeletal muscle development. These differences may be a product of Panx3 having other important roles in skeletal muscle *in vivo*, which would not be reflected in myoblast differentiation and proliferation assays. Alternatively, the onset of expression of the low MM species of Panx3, related with the transition of myoblasts from proliferation to early differentiation, may largely precede even the earliest time point assessed in our *in vivo* assays. Furthermore, it is possible that some of the variations noted may in part be due to species differences between humans and mice. However, our results do indicate that the low MM species of Panx3 gradually increases during muscle regeneration. Following damage of myofibers, quiescent SCs are activated to enter the cell cycle and proliferate, allowing the expansion of the myogenic cell population [175]. Since our data indicate that SCs also express Panx3, it is possible that the increase of the lower MM species of Panx3 seen during regeneration is due to an elevation of Panx3 expression in SCs to promote their differentiation. Our findings also indicate that human SCs express much higher levels of the ~70 kDa immunoreactive species of Panx3 than do differentiated myoblasts. Since our previous work showed that reduction of the ~70 kDa immunoreactive species of PANX3 expression using shRNAs did not affect myoblast differentiation but resulted in significant inhibition of their proliferation [14], its high levels in embryonic and postnatal skeletal muscles as well as in degenerated muscles likely contribute to SC proliferation, which is necessary for muscle growth and repair. As growth is less prominent in the mature or fully regenerated muscle, it was thus expected that the levels of the ~70 kDa immunoreactive species of Panx3 would be significantly lower in developing or regenerating tissue. While this report did not look at the role of PANX3 in human SCs, I

predict that the lower MM species of PANX3 will remain at relatively low levels during human SC differentiation *in vitro* as proliferative myoblasts and likely proliferative SCs express mainly the ~70 kDa immunoreactive form of PANX3 (dotted green line), while differentiated skeletal muscle more prominently express the lower MM form of Panx3 (dotted orange line) and express decreased levels of the ~70 kDa immunoreactive species of Panx3 (**Fig. 19**). Future studies could look at Panx3/PANX3 levels during SC differentiation and whether modulating their levels affect SC differentiation and proliferation. Possible mechanistic pathways to explore include Wnt signalling and intracellular Ca^{2+} signalling. Wnt signalling has been shown to promote the proliferation of osteoprogenitors [185] as well as the proliferation of SCs isolated from mice *in vitro* and during regeneration, specifically Wnt1, Wnt3a or Wnt5a [186]. Increases of intracellular Ca^{2+} has been shown to induce osteoblast differentiation through ER Panx3 channels and P_2X signalling downstream [28], while Ca^{2+} signaling has been reported to induce SC activation and proliferation during regeneration [187–191]. Altogether these results suggest that Panx1/PANX1 and Panx3/PANX3 contribute to the fine balance between proliferation and differentiation *in vitro*, and the regulation of myogenesis *in vivo*.

In mature murine skeletal muscles, we found here that Panx1 and Panx3 are differentially expressed amongst skeletal muscle types. While all muscles assessed expressed Panx1, its levels were higher in slow-twitch muscle (SOL) than in fast-twitch muscles (TA and EDL). In accordance with our data, Panx1 labelling in rat skeletal muscles was present in the interior of both fast- and slow-twitch muscle fibers [150]. Panx1 was shown to be located in a region of the T-tubule membrane [149,150], consistent with a stronger labelling near the sarcolemma. Interestingly, ATP signalling is known to be

involved in the potentiation of both fast- and slow-twitch muscle contraction [150]. It has been demonstrated that the ATP required for potentiation response of rat EDL and SOL contraction is released via Panx1 channels [150]. Importantly, SOL muscles of Panx1 KO mice did not show potentiation of the contraction response [150]. The lost potentiation response of skeletal muscles in Panx1 KO mice could be reversed by the addition of exogenous ATP, confirming that Panx1 channels are necessary for the potentiation response through the release of ATP [27]. In addition to inhibiting ATP release, Panx1 channel blockade using ^{10}Panx peptide strongly reduced a fast calcium signal associated with contraction and a slow signal that regulates gene expression in skeletal myotubes [151]. The ATP released mediated by Panx1 channels after electrical stimulation was shown to play a key role in transcription of the slow-type troponin (TnI) gene [149], a signature of the fast-to-slow muscle fiber phenotype transition [157]. Panx1 was also recently shown to be part of a multiprotein complex, involving DHPR, P_2Y_2 receptor, dystrophin, and caveolin-3, relevant to the E-T coupling process in rodent skeletal muscle cells [152]. In addition to their role in the potentiation of contraction and skeletal muscle plasticity, *Cea et al.* proposed that Panx1 channels may also help maintain the normal oxidative state of skeletal muscle [159]. Indeed, absence of Panx1 (in KO mice) prevented increase in ROS induced by skeletal muscle denervation [159]. Skeletal muscle responds to exercise or electrical stimuli with an increased generation of ROS [158]. It was demonstrated that the increase in ROS production induced by electrical stimulation could be blocked by carbenoxolone [158]. This effect was mimicked by exogenous ATP suggesting that ATP released via Panx1 channels during electrical stimulation is necessary to increase ROS production during depolarization of skeletal muscle fibers [158]. Altogether these data

suggest that Panx1 channels are important to adult skeletal muscle health by regulating the potentiation of the contractile response, muscle plasticity that enables adaptation to demand, and the oxidative state during exercise or electrical stimuli.

While some studies have investigated possible functions of Panx1 in skeletal muscle, little is known about Panx3. Here we have shown that, as opposed to Panx1, the lower MM species of Panx3 was more abundant in the fast-twitch EDL muscle than in the slow-twitch SOL muscle which may suggest different functions for Panx1 and Panx3. Interestingly Panx3 channels have been shown to be involved in ATP release from rat L6 skeletal muscle myotubes [163], as well as to function as a Ca^{2+} channel in the endoplasmic reticulum of osteoblasts and osteoprogenitor cells, and primary calvarial cells [28,185,192]. Since Ca^{2+} plays a central role in skeletal muscle function and plasticity by regulating contraction, metabolism, and activity-dependant adaptation [193], Panx3 channels may thus have a pivotal role in these processes. While Panx3 KO mice have yet to be studied in terms of their skeletal muscle phenotype and function, a recent study on the effect of the global deletion of Panx3 on long bone morphology noted that Panx3 KO mice had larger areas of muscle attachment than wild-type mice, suggesting a possible skeletal muscle defect [164]. Another avenue of research is to study whether Panx1/PANX1 and Panx3/PANX3 are involved in fast-to-slow twitch transition as previously discussed possibly through function of SCs specifically, given that fast twitch fibers are preferentially affected in DMD [127–129], transitioning dystrophic muscle from fast-to-slow fiber type is proposed to confer some protection from disease pathology [194], and SCs have been demonstrated to be more abundant in slow-twitch fibers and facilitate this fast-to-slow twitch transition [195–197].

In the present work, we have also found a differential regulation between Panx1 and Panx3 levels in muscular dystrophy (summarized in **Fig. 19**). Panx1 levels were not significantly altered in *mdx* skeletal muscles as only a small reduction was observed in dystrophic EDL muscle, but not in TA and SOL muscles. Similar results have been obtained using heart homogenates from *mdx* mice [198]. Despite this, Panx1 levels were elevated in triad-enriched fractions (T-tubule/sarcoplasmic reticulum junctional complexes) from back and limb muscles of *mdx* mice [161], suggesting that the effect of dystrophy on Panx1 levels may differ amongst muscle types. Accordingly, Panx1 levels were significantly reduced in EDL and SOL muscles as well as in the diaphragm of *dKO* mice, but not in TA muscles. It is also possible that specific regulation of Panx1 levels occurs within unique cell compartments, such as the T-tubules/sarcoplasmic reticulum, in dystrophic versus healthy skeletal muscle cells. Nevertheless, Panx1 channels have been suggested as the primary route of ATP release in *mdx* and normal skeletal muscle fibers [161]. Interestingly, *Valladares et al.* found that the basal levels of extracellular ATP were higher in fibers from *flexor digitorum brevis* of *mdx* mice compared to normal fibers; however, this release was not dependent on membrane depolarization [161]. Interestingly, dystrophin has been identified as part of the multiprotein complex with Panx1 involved in E-T coupling, thus implicating Panx1 in muscle dystrophy. Furthermore, E-T coupling was found to be altered in *mdx* muscle fibers, which may be due to a decreased association between Cav1.1 and Panx1 following either destabilization of the plasma membrane due to dystrophin deficiency, or a change in the relative amounts of Cav1.1 and Panx1 [161]. Interestingly, while ATP release was demonstrated to have an anti-apoptotic effect in normal fibers, exogenous ATP induced an increase in the expression

of pro-apoptotic genes in dystrophic fibers, which could contribute to fiber loss in DMD [161]. However, exogenous ATP induced an increase in the expression of pro-apoptotic genes in dystrophic fibers, which could participate in the loss of fibers in DMD [161]. While deregulation of Panx1 channel activity may not be linked to heart failure in DMD as treatment with [10]Panx did not affect the isoproterenol-induced lethality in *mdx* and *dKO* mice, Panx1 channels may still be involved in the muscle fragility, reduced muscle strength, contraction-induced damage, and fiber necrosis or fiber loss seen in DMD. Given that the diaphragm is also subject to extensive fiber necrosis, Panx1 channel blockage could possibly inhibit the ATP-induced expression of pro-apoptotic genes, preventing diaphragm fiber loss and subsequent respiratory muscle failure. As mentioned above, it would also be interesting to study the role of Panx1/PANX1 in SC self-renewal and commitment as differential observations were seen in SCs compared to myoblasts during differentiation and proliferation, and DMD is partially described as a disease of impaired SC asymmetric division [115,121].

With respect to Panx3, its levels were also significantly altered in all *dKO* muscles examined with its low MM species being decreased and its ~70 kDa immunoreactive species being strikingly elevated. While little known in regards to the potential roles of Panx3 in skeletal muscle health and disease, it has been reported that nucleotides released from palmitate-challenged muscle cells through Panx3 attracts monocytes suggesting a role for Panx3 in immune cell chemoattraction toward muscle in the context of obesity [163]. Nevertheless, whether or not Panx3 is involved in the promotion of DMD by recruiting inflammatory monocytes [199] or through another mechanism remains to be investigated. Increased Panx1 and Panx3 levels were observed

in areas of muscle associated to inflammation and necrosis during dystrophy, but further work is required to confirm whether Panx1 and Panx3 levels are truly increased in inflammatory cells such as macrophages and neutrophils in *dKO* muscle, which is beyond the scope of this report. Moreover, it is not yet known whether these dysregulated levels of Panx1 and Panx3 in dystrophic mice reflect impaired differentiation and proliferation of myoblasts and SCs *in vitro,* and whether modulating Panx1/PANX1 and Panx3/PANX3 levels or channel function will rescue these cellular processes as well as regeneration in dystrophic models.

Together with our previous findings that Panx1 and Panx3 channels are novel regulators of myoblast proliferation and differentiation, our data that Panx1 and Panx3 channels are also expressed in SCs, that Panx1 and Panx3 levels are tightly regulated during skeletal muscle development, regeneration, and Duchenne muscular dystrophy, and that PANX1 may play important roles in human SC differentiation and proliferation suggest that Panx1/PANX1 and Panx3/PANX3 channels play an important role in skeletal muscle health and disease. Future work is necessary to confirm whether Panx1/PANX1 is involved in skeletal muscle regeneration and dystrophy, by using Panx1 channel blockers such as probenecid, carbenoxolone or ^{10}Panx mimetic peptide ^{50} during CTX degeneration/regeneration experiments *in vivo* on wild-type mice or on dystrophic mice to observe whether regeneration is affected or disease progression is exacerbated. On the other hand, studying the role of Panx3/PANX3 on skeletal muscle regeneration and dystrophy *in vivo* will require Panx3 KO mice as no Panx3 channel blockers have been reported in literature. Moreover, potential functional redundancy may occur between Panxs, thus enabling compensation. As such, interfering Panx channel

expression using Panx knockout mice (Panx1 KO; Panx3 KO; and Panx1/Panx3 dKO) to specifically investigate the roles of both Panx1 and Panx3 in skeletal muscle regeneration and dystrophy as well as development *in vivo* will be crucial, especially since Panx1 and Panx3 KO mice have not yet been assessed in this context.

REFERENCES

1. Panchina, Y. *et al.* A ubiquitous family of putative gap junction molecules. *Current Biology* **10,** R473–R474 (2000).
2. Bruzzone, R., Hormuzdi, S. G., Barbe, M. T., Herb, A. & Monyer, H. Pannexins, a family of gap junction proteins expressed in brain. *Proc. Natl. Acad. Sci. U. S. A.* **100,** 13644–9 (2003).
3. Baranova, A. *et al.* The mammalian pannexin family is homologous to the invertebrate innexin gap junction proteins. *Genomics* **83,** 706–716 (2004).
4. Penuela, S. *et al.* Pannexin 1 and pannexin 3 are glycoproteins that exhibit many distinct characteristics from the connexin family of gap junction proteins. *J. Cell Sci.* **120,** 3772–3783 (2007).
5. Celetti, S. J. *et al.* Implications of pannexin 1 and pannexin 3 for keratinocyte differentiation. *J. Cell Sci.* **123,** 1363–1372 (2010).
6. Penuela, S., Celetti, S. J., Bhalla, R., Shao, Q. & Laird, D. W. Diverse Subcellular Distribution Profiles of Pannexin1 and Pannexin3. *Cell Commun. Adhes.* **15,** 133–142 (2008).
7. Ransford, G. A. *et al.* Pannexin 1 contributes to ATP release in airway epithelia. *Am. J. Respir. Cell Mol. Biol.* **41,** 525–34 (2009).
8. Pelegrin, P. & Surprenant, A. Pannexin-1 mediates large pore formation and interleukin-1beta release by the ATP-gated P2X7 receptor. *EMBO J.* **25,** 5071–82 (2006).
9. Vogt, A., Hormuzdi, S. G. & Monyer, H. *Pannexin1 and Pannexin2 expression in the developing and mature rat brain*. *Molecular Brain Research* **141,** (2005).
10. Boassa, D., Nguyen, P., Hu, J., Ellisman, M. H. & Sosinsky, G. E. Pannexin2 oligomers localize in the membranes of endosomal vesicles in mammalian cells while Pannexin1 channels traffic to the plasma membrane. *Front. Cell. Neurosci.* **8,** 468 (2014).
11. Le Vasseur, M., Lelowski, J., Bechberger, J. F., Sin, W.-C. & Naus, C. C. Pannexin 2 protein expression is not restricted to the CNS. *Front. Cell. Neurosci.* **8,** 1–13 (2014).
12. Bond, S. R. *et al.* Pannexin 3 is a novel target for Runx2, expressed by osteoblasts and mature growth plate chondrocytes. *J. Bone Miner. Res.* **26,** 2911–2922 (2011).
13. Iwamoto, T. *et al.* Pannexin 3 regulates intracellular ATP/cAMP levels and promotes chondrocyte differentiation. *J. Biol. Chem.* **285,** 18948–18958 (2010).
14. Langlois, S. *et al.* Pannexin 1 and Pannexin 3 Channels Regulate Skeletal Muscle Myoblast Proliferation and Differentiation. *J. Biol. Chem.* **289,** 30717–30731

(2014).
15. Li, S., Tomić, M. & Stojilkovic, S. S. Characterization of novel Pannexin 1 isoforms from rat pituitary cells and their association with ATP-gated P2X channels. *Gen. Comp. Endocrinol.* **174,** 202–210 (2011).
16. Turmel, P. *et al.* Characterization of pannexin1 and pannexin3 and their regulation by androgens in the male reproductive tract of the adult rat. *Mol. Reprod. Dev.* **78,** 124–138 (2011).
17. Zoidl, G., Kremer, M., Zoidl, C., Bunse, S. & Dermietzel, R. Molecular Diversity of Connexin and Pannexin Genes in the Retina of the Zebrafish *Danio rerio*. *Cell Commun. Adhes.* **15,** 169–183 (2008).
18. Bond, S. R. & Naus, C. C. The pannexins: Past and present. *Front. Physiol.* **5 FEB,** 1–24 (2014).
19. Yen, M. & Saierjr, M. Gap junctional proteins of animals: The innexin/pannexin superfamily. *Prog. Biophys. Mol. Biol.* **94,** 5–14 (2007).
20. Penuela, S., Gehi, R. & Laird, D. W. The biochemistry and function of pannexin channels. *Biochim. Biophys. Acta - Biomembr.* **1828,** 15–22 (2013).
21. Boassa, D. *et al.* Pannexin1 channels contain a glycosylation site that targets the hexamer to the plasma membrane. *J. Biol. Chem.* **282,** 31733–31743 (2007).
22. Cowan, K. N., Langlois, S., Penuela, S., Cowan, B. J. & Laird, D. W. Pannexin1 and Pannexin3 Exhibit Distinct Localization Patterns in Human Skin Appendages and are Regulated during Keratinocyte Differentiation and Carcinogenesis. *Cell Commun. Adhes.* **19,** 45–53 (2012).
23. Penuela, S., Bhalla, R., Nag, K. & Laird, D. W. Glycosylation regulates Panx intermixing and cellular localization. 4313–4323 (2009).
24. Bruzzone, R., Barbe, M. T., Jakob, N. J. & Monyer, H. Pharmacological properties of homomeric and heteromeric pannexin hemichannels expressed in Xenopus oocytes. *J. Neurochem.* **92,** 1033–1043 (2005).
25. Locovei, S., Bao, L. & Dahl, G. Pannexin 1 in erythrocytes: function without a gap. *Proc. Natl. Acad. Sci. U. S. A.* **103,** 7655–9 (2006).
26. Locovei, S., Scemes, E., Qiu, F., Spray, D. C. & Dahl, G. Pannexin1 is part of the pore forming unit of the P2X(7) receptor death complex. *FEBS Lett.* **581,** 483–8 (2007).
27. Cea, L. A., Riquelme, M. A., Vargas, A. A., Urrutia, C. & Sáez, J. C. Pannexin 1 channels in skeletal muscles. *Front. Physiol.* **5,** 139 (2014).
28. Ishikawa, M. *et al.* Pannexin 3 functions as an ER Ca 2+ channel, hemichannel, and gap junction to promote osteoblast differentiation. *J. Cell Biol.* **193,** 1257–1274 (2011).
29. Lai, C. P. K. *et al.* Tumor-Suppressive Effects of Pannexin 1 in C6 Glioma Cells. *Cancer Res.* **67,** (2007).
30. Locovei, S., Wang, J. & Dahl, G. *Activation of pannexin 1 channels by ATP through P2Y receptors and by cytoplasmic calcium*. *FEBS Letters* **580,** (2006).
31. Orellana, J. A. *et al.* ATP and glutamate released via astroglial connexin 43 hemichannels mediate neuronal death through activation of pannexin 1 hemichannels. *J. Neurochem.* **118,** 826–840 (2011).
32. Sandilos, J. K. *et al.* Pannexin 1, an ATP release channel, is activated by caspase cleavage of its pore-associated C-terminal autoinhibitory region. *J. Biol. Chem.*

287, 11303–11 (2012).
33. Scemes, E. & Spray, D. C. Extracellular K^+ and astrocyte signaling via connexin and pannexin channels. *Neurochem. Res.* **37,** 2310–6 (2012).
34. Chekeni, F. B. *et al.* Pannexin 1 channels mediate 'find-me' signal release and membrane permeability during apoptosis. *Nature* **467,** 863–7 (2010).
35. Silverman, W. R. *et al.* The pannexin 1 channel activates the inflammasome in neurons and astrocytes. *J. Biol. Chem.* **284,** 18143–51 (2009).
36. Wang, J., Ma, M., Locovei, S., Keane, R. W. & Dahl, G. Modulation of membrane channel currents by gap junction protein mimetic peptides: size matters. *Am. J. Physiol. - Cell Physiol.* **293,** (2007).
37. Bhaskaracharya, A. *et al.* Probenecid blocks human P2X7 receptor-induced dye uptake via a pannexin-1 independent mechanism. *PLoS One* **9,** 3–10 (2014).
38. Silverman, W., Locovei, S. & Dahl, G. Probenecid, a gout remedy, inhibits pannexin 1 channels. *Am. J. Physiol. Cell Physiol.* **295,** C761-7 (2008).
39. Michalski, K. & Kawate, T. Carbenoxolone inhibits Pannexin1 channels through interactions in the first extracellular loop. *J. Gen. Physiol.* **147,** 165–74 (2016).
40. Prochnow, N. *et al.* Pannexin1 Stabilizes Synaptic Plasticity and Is Needed for Learning. *PLoS One* **7,** e51767 (2012).
41. Ardiles, A. O. *et al.* Pannexin 1 regulates bidirectional hippocampal synaptic plasticity in adult mice. *Front. Cell. Neurosci.* **8,** 326 (2014).
42. Begandt, D. *et al.* Pannexin channel and connexin hemichannel expression in vascular function and inflammation. *BMC Cell Biol.* **18,** 2 (2017).
43. Makarenkova, H. P. & Shestopalov, V. I. The role of pannexin hemichannels in inflammation and regeneration. *Front. Physiol.* **5 FEB,** 1–8 (2014).
44. Crespo Yanguas, S. *et al.* Pannexin1 as mediator of inflammation and cell death. *Biochim. Biophys. Acta - Mol. Cell Res.* **1864,** 51–61 (2017).
45. Qu, Y. *et al.* Pannexin-1 is Required for ATP Release during Apoptosis but Not for Inflammasome Activation. 6553–6561 (2011).
46. Oh, S.-K. *et al.* Pannexin 3 is required for normal progression of skeletal development in vertebrates. *FASEB J.* **29,** 4473–84 (2015).
47. Ishikawa, M. & Yamada, Y. The Role of Pannexin 3 in Bone Biology. *J. Dent. Res.* **96,** 372–379 (2017).
48. Shao, Q. *et al.* A Germline Variant in the PANX1 Gene Has Reduced Channel Function and Is Associated with Multisystem Dysfunction. *J. Biol. Chem.* **291,** 12432–43 (2016).
49. Furlow, P. W. *et al.* Mechanosensitive pannexin-1 channels mediate microvascular metastatic cell survival. *Nat. Cell Biol.* **17,** 943–52 (2015).
50. Thompson, R. J. *et al.* Activation of Pannexin-1 Hemichannels Augments Aberrant Bursting in the Hippocampus. *Science (80-.).* **322,** 1555–1559 (2008).
51. Lutz, S. E. *et al.* Contribution of pannexin1 to experimental autoimmune encephalomyelitis. *PLoS One* **8,** e66657 (2013).
52. Thompson, R. J., Zhou, N. & MacVicar, B. A. Ischemia Opens Neuronal Gap Junction Hemichannels. *Science (80-.).* **312,** (2006).
53. Gulbransen, B. D. & Sharkey, K. A. Novel functional roles for enteric glia in the gastrointestinal tract. *Nat. Rev. Gastroenterol. Hepatol.* **9,** 625–632 (2012).
54. Orellana, J. A., Retamal, M. A., Moraga-Amaro, R. & Stehberg, J. Role of

Astroglial Hemichannels and Pannexons in Memory and Neurodegenerative Diseases. *Front. Integr. Neurosci.* **10,** 26 (2016).
55. Diezmos, E. F., Bertrand, P. P. & Liu, L. Purinergic Signaling in Gut Inflammation: The Role of Connexins and Pannexins. *Front. Neurosci.* **10,** 311 (2016).
56. Moon, P. M. *et al.* Deletion of Panx3 Prevents the Development of Surgically Induced Osteoarthritis. *J. Mol. Med. (Berl).* **93,** 845–56 (2015).
57. Halliwill, K. D. *et al.* Panx3 links body mass index and tumorigenesis in a genetically heterogeneous mouse model of carcinogen-induced cancer. *Genome Med.* **8,** 1–17 (2016).
58. Buckingham, M. *et al.* The formation of skeletal muscle: from somite to limb. *J. Anat.* **202,** 59–68 (2003).
59. Shi, X. & Garry, D. J. Muscle stem cells in development, regeneration, and disease. *Genes Dev.* **20,** 1692–1708 (2006).
60. Rudnicki, M. A. *et al.* MyoD or Myf-5 is required for the formation of skeletal muscle. *Cell* **75,** 1351–9 (1993).
61. Charge, S. B. & Rudnicki, M. A. Cellular and molecular regulation of muscle regeneration. *Physiol Rev* **84,** 209–238 (2004).
62. Konigsberg, I. R. Clonal analysis of myogenesis. *Science* **140,** 1273–84 (1963).
63. Snow, M. H. Myogenic cell formation in regenerating rat skeletal muscle injured by mincing II. An autoradiographic study. *Anat. Rec.* **188,** 201–217 (1977).
64. Yaffe, D. Cellular aspects of muscle differentiation in vitro. *Curr. Top. Dev. Biol.* **4,** 37–77 (1969).
65. Bischoff, R. Regeneration of single skeletal muscle fibers in vitro. *Anat. Rec.* **182,** 215–235 (1975).
66. Konigsberg, U. R., Lipton, B. H. & Konigsberg, I. R. The regenerative response of single mature muscle fibers isolated in vitro. *Dev. Biol.* **45,** 260–75 (1975).
67. Mauro, A. Satellite cell of skeletal muscle fibers. *J. Biophys. Biochem. Cytol.* **9,** 493–5 (1961).
68. Tajbakhsh, S. & Buckingham, M. The birth of muscle progenitor cells in the mouse: spatiotemporal considerations. *Curr. Top. Dev. Biol.* **48,** 225–68 (2000).
69. Christ, B. & Ordahl, C. P. Early stages of chick somite development. *Anat. Embryol. (Berl).* **191,** 381–96 (1995).
70. Bober, E., Franz, T., Arnold, H. H., Gruss, P. & Tremblay, P. Pax-3 is required for the development of limb muscles: a possible role for the migration of dermomyotomal muscle progenitor cells. *Development* **120,** (1994).
71. Buckingham, M. & Relaix, F. The Role of Pax Genes in the Development of Tissues and Organs: Pax3 and Pax7 Regulate Muscle Progenitor Cell Functions. *Annu. Rev. Cell Dev. Biol.* **23,** 645–673 (2007).
72. Buckingham, M. & Rigby, P. W. J. Gene Regulatory Networks and Transcriptional Mechanisms that Control Myogenesis. *Dev. Cell* **28,** 225–238 (2014).
73. Hutcheson, D. A., Zhao, J., Merrell, A., Haldar, M. & Kardon, G. Embryonic and fetal limb myogenic cells are derived from developmentally distinct progenitors and have different requirements for beta-catenin. *Genes Dev.* **23,** 997–1013 (2009).
74. Hasty, P. *et al.* Muscle deficiency and neonatal death in mice with a targeted

mutation in the myogenin gene. *Nature* **364,** 501–506 (1993).
75. Millay, D. P. *et al.* Myomaker is a membrane activator of myoblast fusion and muscle formation. *Nature* **499,** 301–5 (2013).
76. Uruno, T. *et al.* Distinct regulation of myoblast differentiation by intracellular and extracellular fibroblast growth factor-1. *Growth Factors* **17,** 93–113 (1999).
77. Charvet, C. *et al.* New role for serum response factor in postnatal skeletal muscle growth and regeneration via the interleukin 4 and insulin-like growth factor 1 pathways. *Mol. Cell. Biol.* **26,** 6664–74 (2006).
78. Elia, D., Madhala, D., Ardon, E., Reshef, R. & Halevy, O. Sonic hedgehog promotes proliferation and differentiation of adult muscle cells: Involvement of MAPK/ERK and PI3K/Akt pathways. *Biochim. Biophys. Acta - Mol. Cell Res.* **1773,** 1438–1446 (2007).
79. von Maltzahn, J., Renaud, J.-M., Parise, G. & Rudnicki, M. A. Wnt7a treatment ameliorates muscular dystrophy. *Proc. Natl. Acad. Sci. U. S. A.* **109,** 20614–9 (2012).
80. von Maltzahn, J., Chang, N. C., Bentzinger, C. F. & Rudnicki, M. A. Wnt signaling in myogenesis. *Trends Cell Biol.* **22,** 602–9 (2012).
81. Seward, D. J., Haney, J. C., Rudnicki, M. A. & Swoap, S. J. bHLH transcription factor MyoD affects myosin heavy chain expression pattern in a muscle-specific fashion. *Am. J. Physiol. - Cell Physiol.* **280,** (2001).
82. Gunn, H. M. Differences in the histochemical properties of skeletal muscles of different breeds of horses and dogs. *J. Anat.* **127,** 615–34 (1978).
83. Bröhl, D. *et al.* Colonization of the Satellite Cell Niche by Skeletal Muscle Progenitor Cells Depends on Notch Signals. *Dev. Cell* **23,** 469–481 (2012).
84. Schiaffino, S. & Reggiani, C. Fiber types in mammalian skeletal muscles. *Physiol. Rev.* **91,** 1447–531 (2011).
85. Guth, L. & Samaha, F. J. Qualitative differences between actomyosin ATPase of slow and fast mammalian muscle. *Exp. Neurol.* **25,** 138–152 (1969).
86. Smerdu, V., Karsch-Mizrachi, I., Campione, M., Leinwand, L. & Schiaffino, S. Type IIx myosin heavy chain transcripts are expressed in type IIb fibers of human skeletal muscle. *Am. J. Physiol.* **267,** C1723-8 (1994).
87. Peter, J. B., Barnard, R. J., Edgerton, V. R., Gillespie, C. A. & Stempel, K. E. Metabolic profiles of three fiber types of skeletal muscle in guinea pigs and rabbits. *Biochemistry* **11,** 2627–33 (1972).
88. Kammoun, M., Cassar-Malek, I., Meunier, B. & Picard, B. A simplified immunohistochemical classification of skeletal muscle fibres in mouse. *Eur. J. Histochem.* **58,** 2254 (2014).
89. Soukup, T., Zachařová, G. & Smerdu, V. Fibre type composition of soleus and extensor digitorum longus muscles in normal female inbred Lewis rats. *Acta Histochem.* **104,** 399–405 (2002).
90. Guido, A. N., Campos, G. E. R., Neto, H. S., Marques, M. J. & Minatel, E. Fiber Type Composition of the Sternomastoid and Diaphragm Muscles of Dystrophin-Deficient mdx Mice. *Anat. Rec. Adv. Integr. Anat. Evol. Biol.* **293,** 1722–1728 (2010).
91. Meznaric, M. & Cvetko, E. Size and Proportions of Slow-Twitch and Fast-Twitch Muscle Fibers in Human Costal Diaphragm. *Biomed Res. Int.* **2016,** 5946520

(2016).
92. Gutiérrez, J. M., Chaves, F., Mata, E. & Cerdas, L. Skeletal muscle regeneration after myonecrosis induced by Bothrops asper (terciopelo) venom. *Toxicon* **24,** 223–31 (1986).
93. Imbert, N., Cognard, C., Duport, G., Guillou, C. & Raymond, G. Abnormal calcium homeostasis in Duchenne muscular dystrophy myotubes contracting in vitro. *Cell Calcium* **18,** 177–86 (1995).
94. Alderton, J. M. & Steinhardt, R. A. Calcium influx through calcium leak channels is responsible for the elevated levels of calcium-dependent proteolysis in dystrophic myotubes. *J. Biol. Chem.* **275,** 9452–60 (2000).
95. Tatsumi, R., Anderson, J. E., Nevoret, C. J., Halevy, O. & Allen, R. E. HGF/SF Is Present in Normal Adult Skeletal Muscle and Is Capable of Activating Satellite Cells. *Dev. Biol.* **194,** 114–128 (1998).
96. Lefaucheur, J. P. & Sebille, A. Basic fibroblast growth factor promotes in vivo muscle regeneration in murine muscular dystrophy. *Neurosci. Lett.* **202,** 121–124 (1995).
97. Lefaucheur, J.-P. & Sébille, A. Muscle regeneration following injury can be modified in vivo by immune neutralization of basic fibroblast growth factor, transforming growth factor β1 or insulin-like growth factor I. *J. Neuroimmunol.* **57,** 85–91 (1995).
98. Floss, T., Arnold, H. H. & Braun, T. A role for FGF-6 in skeletal muscle regeneration. *Genes Dev.* **11,** 2040–51 (1997).
99. Rappolee, D. A. & Werb, Z. Macrophage-derived growth factors. *Curr. Top. Microbiol. Immunol.* **181,** 87–140 (1992).
100. Fielding, R. A. *et al.* Acute phase response in exercise. III. Neutrophil and IL-1 beta accumulation in skeletal muscle. *Am. J. Physiol. - Regul. Integr. Comp. Physiol.* **265,** (1993).
101. Orimo, S., Hiyamuta, E., Arahata, K. & Sugita, H. Analysis of inflammatory cells and complement C3 in bupivacaine-induced myonecrosis. *Muscle Nerve* **14,** 515–520 (1991).
102. Tidball, J. G. Inflammatory cell response to acute muscle injury. *Med Sci Sport. Exerc* **27,** 1022–1032 (1995).
103. Zammit, P. S. *et al.* Muscle satellite cells adopt divergent fates: a mechanism for self-renewal? *J. Cell Biol.* **166,** 347–57 (2004).
104. Seale, P. Pax7 Is Required for the Specification of Myogenic Satellite Cells. *Cell* **102,** 777–786 (2000).
105. Kuang, S. Distinct roles for Pax7 and Pax3 in adult regenerative myogenesis. *J. Cell Biol.* **172,** 103–113 (2006).
106. Kassar-Duchossoy, L. *et al.* Pax3/Pax7 mark a novel population of primitive myogenic cells during development. *Genes Dev.* **19,** 1426–31 (2005).
107. Olguin, H. C. & Olwin, B. B. Pax-7 up-regulation inhibits myogenesis and cell cycle progression in satellite cells: a potential mechanism for self-renewal. *Dev. Biol.* **275,** 375–88 (2004).
108. von Maltzahn, J., Jones, A. E., Parks, R. J. & Rudnicki, M. A. Pax7 is critical for the normal function of satellite cells in adult skeletal muscle. *Proc. Natl. Acad. Sci. U. S. A.* **110,** 16474–9 (2013).

109. Schultz, E., Jaryszak, D. L. & Valliere, C. R. Response of satellite cells to focal skeletal muscle injury. *Muscle Nerve* **8,** 217–222 (1985).
110. Wang, J. & Conboy, I. Embryonic vs. Adult Myogenesis: Challenging the 'Regeneration Recapitulates Development' Paradigm. *J. Mol. Cell Biol.* **2,** 1–4 (2010).
111. Kuang, S., Kuroda, K., Le Grand, F. & Rudnicki, M. A. Asymmetric self-renewal and commitment of satellite stem cells in muscle. *Cell* **129,** 999–1010 (2007).
112. Bischoff, R. Interaction between satellite cells and skeletal muscle fibers. *Development* **109,** 943–52 (1990).
113. Yin, H., Price, F. & Rudnicki, M. A. Satellite cells and the muscle stem cell niche. *Physiol. Rev.* **93,** 23–67 (2013).
114. Troy, A. *et al.* Coordination of satellite cell activation and self-renewal by Par-complex-dependent asymmetric activation of p38α/β MAPK. *Cell Stem Cell* **11,** 541–53 (2012).
115. Dumont, N. A. *et al.* Dystrophin expression in muscle stem cells regulates their polarity and asymmetric division. *Nat. Med.* **21,** 1455–63 (2015).
116. Ownby, C. L., Fletcher, J. E. & Colberg, T. R. Cardiotoxin 1 from cobra (Naja naja atra) venom causes necrosis of skeletal muscle in vivo. *Toxicon* **31,** 697–709 (1993).
117. d'Albis, a, Couteaux, R., Janmot, C., Roulet, A. & Mira, J. C. Regeneration after cardiotoxin injury of innervated and denervated slow and fast muscles of mammals. Myosin isoform analysis. *Eur. J. Biochem.* **174,** 103–110 (1988).
118. Bushby, K. *et al.* Diagnosis and management of Duchenne muscular dystrophy, part 1: diagnosis, and pharmacological and psychosocial management. *The Lancet Neurology* **9,** 77–93 (2010).
119. Bushby, K. *et al.* Diagnosis and management of Duchenne muscular dystrophy, part 2: implementation of multidisciplinary care. *The Lancet Neurology* **9,** 177–189 (2010).
120. Petrof, B. J., Shrager, J. B., Stedman, H. H., Kelly, A. M. & Sweeney, H. L. Dystrophin protects the sarcolemma from stresses developed during muscle contraction. *Proc. Natl. Acad. Sci. U. S. A.* **90,** 3710–4 (1993).
121. Chang, N. C., Chevalier, F. P. & Rudnicki, M. A. Satellite Cells in Muscular Dystrophy – Lost in Polarity. *Trends Mol. Med.* **22,** 479–496 (2016).
122. Gailly, P. New aspects of calcium signaling in skeletal muscle cells: implications in Duchenne muscular dystrophy. *Biochim. Biophys. Acta* **1600,** 38–44 (2002).
123. Jiang, T. *et al.* Localized expression of specific P2X receptors in dystrophin-deficient DMD and mdx muscle. *Neuromuscul. Disord.* **15,** 225–36 (2005).
124. Blau, H. M., Webster, C. & Pavlath, G. K. Defective myoblasts identified in Duchenne muscular dystrophy. *Proc. Natl. Acad. Sci. U. S. A.* **80,** 4856–60 (1983).
125. Delaporte, C., Dehaupas, M. & Fardeau, M. Comparison between the growth pattern of cell cultures from normal and Duchenne dystrophy muscle. *J. Neurol. Sci.* **64,** 149–60 (1984).
126. Webster, C. & Blau, H. M. Accelerated age-related decline in replicative life-span of Duchenne muscular dystrophy myoblasts: implications for cell and gene therapy. *Somat. Cell Mol. Genet.* **16,** 557–65 (1990).
127. Zacharias, J. M. & Anderson, J. E. Muscle regeneration after imposed injury is

better in younger than older mdx dystrophic mice. *J. Neurol. Sci.* **104,** 190–6 (1991).
128. Webster, C., Silberstein, L., Hays, A. P. & Blau, H. M. Fast muscle fibers are preferentially affected in Duchenne muscular dystrophy. *Cell* **52,** 503–13 (1988).
129. Pedemonte, M., Sandri, C., Schiaffino, S. & Minetti, C. Early Decrease of IIx Myosin Heavy Chain Transcripts in Duchenne Muscular Dystrophy. *Biochem. Biophys. Res. Commun.* **255,** 466–469 (1999).
130. Bulfield, G., Siller, W. G., Wight, P. A. & Moore, K. J. X chromosome-linked muscular dystrophy (mdx) in the mouse. *Proc. Natl. Acad. Sci. U. S. A.* **81,** 1189–92 (1984).
131. Sicinski, P. *et al.* The molecular basis of muscular dystrophy in the mdx mouse: a point mutation. *Science (80-.).* **244,** (1989).
132. Chamberlain, J. S., Metzger, J., Reyes, M., Townsend, D. & Faulkner, J. A. Dystrophin-deficient mdx mice display a reduced life span and are susceptible to spontaneous rhabdomyosarcoma. *FASEB J.* **21,** 2195–204 (2007).
133. Porter, J. D. *et al.* A chronic inflammatory response dominates the skeletal muscle molecular signature in dystrophin-deficient mdx mice. *Hum. Mol. Genet.* **11,** 263–72 (2002).
134. McGreevy, J. W., Hakim, C. H., McIntosh, M. A. & Duan, D. Animal models of Duchenne muscular dystrophy: from basic mechanisms to gene therapy. *Dis. Model. Mech.* **8,** (2015).
135. McDonald, A. A., Hebert, S. L., Kunz, M. D., Ralles, S. J. & McLoon, L. K. Disease course in mdx:utrophin+/- mice: comparison of three mouse models of Duchenne muscular dystrophy. *Physiol. Rep.* **3,** (2015).
136. Deconinck, A. E. *et al.* Utrophin-Dystrophin-Deficient Mice as a Model for Duchenne Muscular Dystrophy. *Cell* **90,** 717–727 (1997).
137. Hoffman, E. P. *et al.* Restoring dystrophin expression in duchenne muscular dystrophy muscle progress in exon skipping and stop codon read through. *Am. J. Pathol.* **179,** 12–22 (2011).
138. Mendell, J. R. *et al.* Gene therapy for muscular dystrophy: Lessons learned and path forward. *Neurosci. Lett.* **527,** 90–99 (2012).
139. Ousterout, D. G. *et al.* Multiplex CRISPR/Cas9-based genome editing for correction of dystrophin mutations that cause Duchenne muscular dystrophy. *Nat. Commun.* **6,** 6244 (2015).
140. Nelson, C. E. *et al.* In vivo genome editing improves muscle function in a mouse model of Duchenne muscular dystrophy. *Science* aad5143 (2015). doi:10.1126/science.aad5143
141. Long, C. *et al.* Postnatal genome editing partially restores dystrophin expression in a mouse model of muscular dystrophy. *Science* aad5725 (2015). doi:10.1126/science.aad5725
142. Sienkiewicz, D., Kulak, W., Okurowska-Zawada, B., Paszko-Patej, G. & Kawnik, K. Duchenne muscular dystrophy: current cell therapies. *Ther. Adv. Neurol. Disord.* **8,** 166–77 (2015).
143. Angelini, C. & Peterle, E. Old and new therapeutic developments in steroid treatment in Duchenne muscular dystrophy. *Acta Myol. myopathies cardiomyopathies Off. J. Mediterr. Soc. Myol.* **31,** 9–15 (2012).

144. Bareja, A. & Billin, A. N. Satellite cell therapy - from mice to men. *Skelet. Muscle* **3,** 2 (2013).
145. Mah, J. K. Current and emerging treatment strategies for Duchenne muscular dystrophy. *Neuropsychiatr. Dis. Treat.* **12,** 1795–807 (2016).
146. Duch M, K. T., M, D., FS, P., H, L. & EM, F. Test of Critical Steps towards a Combined Cell and Gene Therapy Approach for the Treatment of Duchenne Muscular Dystrophy. *J. Mol. Genet. Med.* **9,** 1–5 (2014).
147. Arnett, A. L. *et al.* Adeno-associated viral (AAV) vectors do not efficiently target muscle satellite cells. *Mol. Ther. Methods Clin. Dev.* **1,** 773–779 (2014).
148. Dumont, N. A., Rudnicki, M. A., Rae, C., Morley, J. W. & Leger, J. J. Targeting muscle stem cell intrinsic defects to treat Duchenne muscular dystrophy. *npj Regen. Med.* **1,** 16006 (2016).
149. Jorquera, G. *et al.* Cav1.1 controls frequency-dependent events regulating adult skeletal muscle plasticity. *J. Cell Sci.* **126,** 1189–98 (2013).
150. Riquelme, M. A. *et al.* The ATP required for potentiation of skeletal muscle contraction is released via pannexin hemichannels. *Neuropharmacology* **75,** 594–603 (2013).
151. Buvinic, S. *et al.* ATP released by electrical stimuli elicits calcium transients and gene expression in skeletal muscle. *J. Biol. Chem.* **284,** 34490–505 (2009).
152. Arias-Calderón, M. *et al.* Characterization of a multiprotein complex involved in excitation-transcription coupling of skeletal muscle. *Skelet. Muscle* **6,** 15 (2016).
153. Riquelme, M. A. *et al.* Pannexin channels mediate the acquisition of myogenic commitment in C2C12 reserve cells promoted by P2 receptor activation. *Front. cell Dev. Biol.* **3,** 25 (2015).
154. Sandona, D. *et al.* The T-tubule membrane ATP-operated P2X4 receptor influences contractility of skeletal muscle. *FASEB J.* **19,** 1184–6 (2005).
155. Chin, E. R. *et al.* A calcineurin-dependent transcriptional pathway controls skeletal muscle fiber type. *Genes Dev.* **12,** 2499–509 (1998).
156. Bassel-Duby, R. & Olson, E. N. Signaling Pathways in Skeletal Muscle Remodeling. *Annu. Rev. Biochem.* **75,** 19–37 (2006).
157. Casas, M. *et al.* IP(3)-dependent, post-tetanic calcium transients induced by electrostimulation of adult skeletal muscle fibers. *J. Gen. Physiol.* **136,** 455–67 (2010).
158. Díaz-Vegas, A. *et al.* ROS Production via P2Y1-PKC-NOX2 Is Triggered by Extracellular ATP after Electrical Stimulation of Skeletal Muscle Cells. *PLoS One* **10,** e0129882 (2015).
159. Cea, L. A. *et al.* De novo expression of connexin hemichannels in denervated fast skeletal muscles leads to atrophy. *Proc. Natl. Acad. Sci. U. S. A.* **110,** 16229–34 (2013).
160. Araya, R., Riquelme, M. A., Brandan, E. & Sáez, J. C. The formation of skeletal muscle myotubes requires functional membrane receptors activated by extracellular ATP. (2004). doi:10.1016/j.brainresrev.2004.06.003
161. Valladares, D. *et al.* Electrical stimuli are anti-apoptotic in skeletal muscle via extracellular ATP. Alteration of this signal in Mdx mice is a likely cause of dystrophy. *PLoS One* **8,** e75340 (2013).
162. Young, C. N. J. *et al.* P2X7 purinoceptor alterations in dystrophic mdx mouse

muscles: relationship to pathology and potential target for treatment. *J. Cell. Mol. Med.* **16,** 1026–37 (2012).
163. Pillon, N. J. *et al.* Nucleotides Released From Palmitate-Challenged Muscle Cells Through Pannexin-3 Attract Monocytes. *Diabetes* **63,** (2014).
164. Caskenette, D. Global deletion of Panx3 produces multiple phenotypic effects in mouse humeri and femora. *Masters Clin. Anat. Proj.* **228,** 746–756 (2015).
165. Condrea, E. Membrane-active polypeptides from snake venom: cardiotoxins and haemocytotoxins. *Experientia* **30,** 121–9 (1974).
166. Clow, C. & Jasmin, B. J. Brain-derived Neurotrophic Factor Regulates Satellite Cell Differentiation and Skeletal Muscle Regeneration. 2182–2190 (2010).
167. Ravel-Chapuis, A. *et al.* The RNA-binding protien Staufen1 impairs myogenic differentiation via a c-myc-dependent mechanism. 3765–3778 (2014).
168. Al-Rewashdy, H., Ljubicic, V., Lin, W., Renaud, J.-M. & Jasmin, B. J. Utrophin A is essential in mediating the functional adaptations of mdx mouse muscle following chronic AMPK activation. *Hum. Mol. Genet.* **24,** 1243–1255 (2015).
169. Mancini, A. *et al.* Regulation of myotube formation by the actin-binding factor drebrin. *Skelet. Muscle* **1,** 1–13 (2011).
170. Tenbaum, S. *et al.* Standardized Relative Quantification of Immunofluorescence Tissue Staining. *Protoc. Exch.* (2012). doi:10.1038/protex.2012.008
171. Schwerzmann, K., Hoppeler, H., Kayar, S. R. & Weibel, E. R. *Oxidative capacity of muscle and mitochondria: correlation of physiological, biochemical, and morphometric characteristics*. (The Academy, 1989). at <http://www.pnas.org/content/86/5/1583>
172. Jackman, M. R. & Willis, W. T. Characteristics of mitochondria isolated from type I and type IIb skeletal muscle. *Am. J. Physiol. - Cell Physiol.* **270,** (1996).
173. Baylor, S. M. & Hollingworth, S. Intracellular calcium movements during excitation-contraction coupling in mammalian slow-twitch and fast-twitch muscle fibers. *J. Gen. Physiol.* **139,** 261–72 (2012).
174. Oustanina, S., Hause, G. & Braun, T. Pax7 directs postnatal renewal and propagation of myogenic satellite cells but not their specification. *EMBO J.* **23,** 3430–3439 (2004).
175. Wang, Y. X. & Rudnicki, M. A. Satellite cells, the engines of muscle repair. *Nat. Rev. Mol. Cell Biol.* **13,** 127–33 (2011).
176. Yan, Z. *et al.* Highly Coordinated Gene Regulation in Mouse Skeletal Muscle Regeneration. *J. Biol. Chem.* **278,** 8826–8836 (2003).
177. Miura, P., Thompson, J., Chakkalakal, J. V, Holcik, M. & Jasmin, B. J. The utrophin A 5'-untranslated region confers internal ribosome entry site-mediated translational control during regeneration of skeletal muscle fibers. *J. Biol. Chem.* **280,** 32997–3005 (2005).
178. Fayssoil, A., Nardi, O., Orlikowski, D. & Annane, D. Cardiomyopathy in Duchenne muscular dystrophy: pathogenesis and therapeutics. *Heart Fail. Rev.* **15,** 103–107 (2010).
179. Mosqueira, M., Zeiger, U., F?rderer, M., Brinkmeier, H. & Fink, R. H. Cardiac and Respiratory Dysfunction in Duchenne Muscular Dystrophy and the Role of Second Messengers. *Med. Res. Rev.* **33,** 1174–1213 (2013).
180. Gnocchi, V. F., White, R. B., Ono, Y., Ellis, J. A. & Zammit, P. S. Further

characterisation of the molecular signature of quiescent and activated mouse muscle satellite cells. *PLoS One* **4,** e5205 (2009).
181. Nofziger, D., Miyamoto, A., Lyons, K. M. & Weinmaster, G. Notch signaling imposes two distinct blocks in the differentiation of C2C12 myoblasts. *Development* **126,** 1689–702 (1999).
182. Delfini, M. C., Hirsinger, E., Pourquié, O. & Duprez, D. Delta 1-activated notch inhibits muscle differentiation without affecting Myf5 and Pax3 expression in chick limb myogenesis. *Development* **127,** 5213–24 (2000).
183. Conboy, I. M., Conboy, M. J., Smythe, G. M. & Rando, T. A. Notch-Mediated Restoration of Regenerative Potential to Aged Muscle. *Science (80-.).* **302,** 1575–1577 (2003).
184. Conboy, I. M. *et al.* Rejuvenation of aged progenitor cells by exposure to a young systemic environment. *Nature* **433,** 760–764 (2005).
185. Ishikawa, M., Iwamoto, T., Fukumoto, S. & Yamada, Y. Pannexin 3 inhibits proliferation of osteoprogenitor cells by regulating Wnt and p21 signaling. *J. Biol. Chem.* **289,** 2839–51 (2014).
186. Otto, A. *et al.* Canonical Wnt signalling induces satellite-cell proliferation during adult skeletal muscle regeneration. *J. Cell Sci.* **121,** 2939–2950 (2008).
187. Sakuma, K. *et al.* Calcineurin is a potent regulator for skeletal muscle regeneration by association with NFATc1 and GATA-2. *Acta Neuropathol.* **105,** 271–80 (2003).
188. Raynaud, F., Carnac, G., Marcilhac, A. & Benyamin, Y. m-Calpain implication in cell cycle during muscle precursor cell activation. *Exp. Cell Res.* **298,** 48–57 (2004).
189. Tu, M. K. & Borodinsky, L. N. Spontaneous calcium transients manifest in the regenerating muscle and are necessary for skeletal muscle replenishment. *Cell Calcium* **56,** 34–41 (2014).
190. Liu, Y. & Schneider, M. F. FGF2 activates TRPC and Ca(2+) signaling leading to satellite cell activation. *Front. Physiol.* **5,** 38 (2014).
191. Tu, M. K., Levin, J. B., Hamilton, A. M. & Borodinsky, L. N. Calcium signaling in skeletal muscle development, maintenance and regeneration. *Cell Calcium* **59,** 91–7 (2016).
192. Ishikawa, M. *et al.* Pannexin 3 and connexin 43 modulate skeletal development via distinct functions and expression patterns. *J. Cell Sci.* jcs.176883- (2016). doi:10.1242/jcs.176883
193. Gehlert, S., Bloch, W. & Suhr, F. Ca2+-Dependent Regulations and Signaling in Skeletal Muscle: From Electro-Mechanical Coupling to Adaptation. *Int. J. Mol. Sci.* **16,** 1066–1095 (2015).
194. Selsby, J. T., Morine, K. J., Pendrak, K., Barton, E. R. & Sweeney, H. L. Rescue of Dystrophic Skeletal Muscle by PGC-1α Involves a Fast to Slow Fiber Type Shift in the mdx Mouse. *PLoS One* **7,** e30063 (2012).
195. Gibson, M. C. & Schultz, E. The distribution of satellite cells and their relationship to specific fiber types in soleus and extensor digitorum longus muscles. *Anat. Rec.* **202,** 329–337 (1982).
196. Gibson, M. C. & Schultz, E. Age-related differences in absolute numbers of skeletal muscle satellite cells. *Muscle Nerve* **6,** 574–580 (1983).

197. Martins, K. J. B. *et al.* Effect of satellite cell ablation on low-frequency-stimulated fast-to-slow fibre-type transitions in rat skeletal muscle. *J. Physiol.* **572,** 281–94 (2006).
198. Gonzalez, Patrick, J., Ramachandran, J., Xie, L.-H., Contreras, J. E. & Fraidenraich, D. Selective Connexin43 Inhibition Prevents Isoproterenol-Induced Arrhythmias and Lethality in Muscular Dystrophy Mice. *Sci. Rep.* **5,** 13490 (2015).
199. Mojumdar, K. *et al.* Inflammatory monocytes promote progression of Duchenne muscular dystrophy and can be therapeutically targeted via CCR2. *EMBO Mol. Med.* **6,** 1476–92 (2014).